ABSTRACT

STUDY OF THE PHOSPHORYLATION OF *PAX6* TRANSACTIVATION DOMAIN *IN VITRO* AND *IN VIVO*

by Peipei Qi

The transcription factor, PAX6, plays essential roles during the development of eyes, brain, and pancreas. Loss of *Pax6* causes complete lack of eye formation in both humans and mice and even prenatal lethality in mice. Heterozygotes for *Pax6* null mutations possess “small eyes” in mice and aniridia in humans. Truncation mutations of human PAX6 C-terminus can also lead to aniridia, demonstrating a critical role of the PAX6 transactivation domain (TAD) during eye formation. Previous studies found that in vitro phosphorylation of the PAX6 TAD by p38 kinase and HIPK2 at seven sites could regulate *Pax6* transactivation. Here, a comprehensive analysis of all thesis phosphorylation sites revealed that PAX6 lost almost all ability to activate transcription when all sites were mutated. Furthermore, phosphorylation of the last site accounts for about 40% of the transcriptional activity and plays the most dominant role among all the phosphorylation sites studied. Additionally, it was proved that TAD phosphorylation could critically regulate *Pax6* transcriptional repression. Together, these in-vitro data demonstrate that PAX6 TAD phosphorylation can strongly affect the dual function of *Pax6* as a trans-activator and trans-repressor. Transgenic mice with sites 2 and 3 mutations exhibited normal eye development, which was consistent with the *in-vitro* data.

STUDY OF THE PHOSPHORYLATION OF PAX6 TRANSACTIVATION DOMAIN *IN VITRO* AND *IN VIVO*

A Thesis

Submitted to the

Faculty of Miami University

in partial fulfillment of

the requirements for the degree of

Master of Science

by

Peipei Qi

Miami University

Oxford, Ohio

2022

Advisor: Michael L. Robinson

Reader: Katia Del Rio-Tsonis

Reader: Haifei Shi

STUDY OF THE PHOSPHORYLATION OF PAX6 TRANSACTIVATION DOMAIN *IN VITRO* AND *IN VIVO*

A Thesis

Submitted to the

Faculty of Miami University

in partial fulfillment of

the requirements for the degree of

Master of Science
by

Peipei Qi

Miami University

Oxford, Ohio

2022

Michael L Robinson

_____

Katia Del Rio-Tsonis

_____

Haifei Shi

_____

Table of Contents

List of Tables

List of Figures

Dedication

I would like to dedicate this work to my husband Huaqun Zhang. He commuted between two cities every other week for more than 4 years. He provided a strong support for my work through what he has done. In addition, I got a sweet baby, Colin Zhang, the most precious gift in my life. Although it was like starting a second PhD program to raise a little baby, he gives me persistent motivation to be a better person. Besides, I lost my grandma last year, and I couldn't even say goodbye to her in person due to the severe pandemic. Some of them just joined the world and some of them have already left me forever. Together, I would like to dedicate my thesis to them all. Without their love and support, I would not be in this position. Without them I would not have the opportunity to keep pursuing my dreams.

Acknowledgements

I would like to thank my wonderful research advisor Dr. Michael L Robinson gratefully and sincerely for his guidance, suggestions, and patience during my graduate studies. As an advisor with a great reputation in the lens field, he is incredibly knowledgeable, kind-hearted, and patient, and he built up my scientific mind and strengthened my ability to deal with challenges via scientific methods. In particular, he always provided me with support and inspiration as much as he could when I was in a difficult time of the research progress. He let me keep trying under a tight lab budget when my project made little progress within nearly three years. Although I eventually failed in pursuing the degree of PhD, it was an absolutely precious and beneficial experience in my whole life. I will keep improving myself by thinking critically and working hard to fight against my spiritual laziness. Furthermore, I also really appreciate the wonderful platform he established. Besides the great impact on research, he also provided me with important support in my life. I still remember the moment when he gave strong encouragement and sincere wishes after I told him I would be a mum, even though everyone knew it would take a great amount of time and attention to raise a baby and my research progress would be affected. I also never forget the long email with the information collected from many people when Mike and Julia (his wife) heard that I was struggling with the search for baby-caring services. He prepared each lab member a sweet card with his kind encouragement and wishes before every Christmas holiday along with a Jungle Jim gift card (once I thought he was a big fan of Jungle Jim). There are so many heart-warming moments that I'm inspired for a long time by their kindness and love. As his student, I learn a lot of valuable qualities from him that will benefit my future career and life.

I would also like to thank the super researcher in Dr. Robinson's lab, Brad Wagner. As senior scientist, he provided a lot of crucial technical support and guidance to my project. He also has a high proficiency in the truly skill-demanding technique of generating transgenic mice, including microinjection, zygote transplantation, and injection of stem cells into blastocysts. My research would not be feasible without his wonderful assistance. Besides, as a super lab manager, he also maintained the lab very well and my research couldn't run smoothly without such an orderly environment.

In addition, I would also like to thank all the other members in the lab, especially Thanh Hoang, Stephanie Padula, Phuong Lam, Anil Upreti, Tycho Jaquish, and Davis Kinkel and many other undergraduate students in our lab for their incredible support and friendship.

I would like to thank all the lab members in Dr. Katia Del Rio-Tsonis's lab, especially Erika Grajales-Esquivel. They have been greatly supportive of my research.

I would like to thank all my committee: Dr. Paul F James, Dr. Haifei Shi, Dr. Katia Del Rio-Tsonis and Dr. Carole Dabney-Smith for their valuable time and fabulous help for my graduate study which has extended my boundaries. In addition, I would like to thank all the staff of the biology department, especially Dr. Thomas Crist and Mrs. Darlene Davidson for their incredible support. I acknowledge and thank the staff at Miami University for instrumentation and technical support.

Last but not least, I would like to thank all of my beloved family members for their endless love, support, and encouragement.

STUDY OF THE PHOSPHORYLATION OF *PAX6* TRANSACTIVATION DOMAIN *IN VITRO* AND *IN VIVO*

Introduction

Pax6 in mammal development

Paired Box 6 (*Pax6*) is a member of the *Pax* gene family and PAX6 protein is a master transcription factor that plays pivotal roles during the development of eye, pancreas and central nervous system (CNS) in vertebrates (Walther and Gruss 1991; Callaerts, Halder, and Gehring 1997; Panneerselvam et al. 2019). The loss of Pax6 leads to lethality during murine embryogenesis. In the clinic, *Pax6* heterozygotes display pan-ocular disorders, such as aniridia, congenital cataract, microcornea, glaucoma and Peters anomaly. Abnormally small eyes are found in mice heterozygous for *Pax6* null mutations and eye formation fails in homozygous *Pax6* null mice (Hill et al. 1991; Machon et al. 2009). In mouse ocular lens development (Fig. 1), *Pax6* is expressed from a very early time point, embryonic day 8.0 (E8.0) in the head surface ectoderm (SE) and the ocular vesicle (OV) where it induces the formation of the lens placode, which subsequently invaginates to form the lens pit that closes off to form the lens vesicle (Goudreau et al. 2002; Cvekl and Ashery-Padan 2014). From E12.5, the posterior cells of the lens vesicle initiate elongation and differentiate into primary lens fiber cells (Kallifatidis et al. 2011). These primary fiber cells fill the lens vesicle and become the embryonic lens nucleus. In the meantime, the anterior cells of the lens vesicle differentiate into lens epithelium, which possesses proliferative ability. Proliferation of lens epithelial cells results in a displacement of cells toward the equator where epithelial cells undergo secondary fiber cell differentiation (Beebe et al. 1982; Piatigorsky 1981). Although the basic anatomy of the lens is formed during embryogenesis, continuous proliferation of lens epithelial cells followed by secondary fiber cell differentiation fuels the growth of the lens throughout the vertebrate lifespan. Cellular and molecular data demonstrate that *Pax6* is essential for the specification of murine lens placode at E9.5 (R. Ashery-Padan et al. 2000) and lens fiber cell differentiation at E14.5 (Shaham et al. 2009). Therefore, ablation of *Pax6* leads to the absence of lens. Also, at the time of lens placode formation, the anterior cells of OV elongate and invaginate into an optic cup (OC) which subsequently differentiates into mouse retina progenitor cells (RPC), that give rise to all cell types of the neural retina. Previous studies have found that murine *Pax6*-deficient RPCs fail to accomplish retina cell differentiation at E10.5 (Klimova and Kozmik 2014). Consequently, reduced retina size is observed in *Pax6*-deficient eyes at E14.5 and morphologically normal retina cells are hardly detected at postnatal day 0 (P0) (Klimova and Kozmik 2014). Thus, *Pax6* is key to retina cell specification.

Besides the essential role in eye development, *Pax6* also can crucially regulate the formation of the mouse CNS. *Pax6* is expressed from the onset of brain development at E8 (Walther and Gruss 1991) to adulthood (Osumi et al. 2008). Inactivation of *Pax6* leads to a severe impairment of neurogenesis, particularly in brain patterning. For instance, in *Sey/Sey* mice (Roberts 1967), loss of *Pax6* disrupted the differential expression of *Gsh2* and *Ngn2* (Toresson, Potter, and Campbell

2000; Yun, Potter, and Rubenstein 2001), and thus severely impaired the establishment of the pallial-subpallial boundary (PSPB), which could critically promote the differentiation of the cerebral cortex and the striatum in normal brain development (Georgala, Carr, and Price 2011). Furthermore, *Pax6* is required to regulate the proliferation of cortical progenitors and abnormally increased number of exit cells cycle resulted in reduced size of cortical progenitor pool in *Pax6*-/- mutated cortex (Quinn et al. 2007). Thus, Pax6 plays multiple critical roles in brain development.

Additionally, *Pax6* also plays an essential role in pancreas formation and is initially detected at E9 in developing mouse pancreas (St-Onge et al. 1997). During differentiation of islet endocrine cells, *Pax6* controls both the number and morphology of endocrine cell types (Sander et al. 1997). Notably, the levels of insulin and glucagon were dramatically reduced in *Pax6* null homozygous mice (Sander et al. 1997; Ruth Ashery-Padan et al. 2004). Besides, conditional inactivation of *Pax6* in 6-month-old mice strongly diminished the expression of *Pdx1*, which acted as a vital regulator of glucose sensing (A. W. Hart et al. 2000). Depletion of *Pax6* led to a great reduction of the production of the endocrine hormones (including insulin, glucagon, and somatostatin) in mature pancreases. Subsequently, typical symptoms of diabetes were found quickly in these mice, suggesting a continued requirement for *Pax6* expression in adult animals (Alan W. Hart et al. 2013). Taken together, *Pax6* plays both a vital role in embryonic development and in regulating normal glucose homeostasis in mammals.

Functional Domains of PAX6

To determine the molecular mechanism underlying PAX6 roles, the biochemical structure of PAX6 has been intensively studied. As a transcription factor, PAX6 harbors two distinct DNA-binding domains, paired domain (PD) and homeodomain (HD). PAX6 also contains a transactivation domain (TAD) at the C-terminus. In the N-terminal region of PAX6, both the PD and the HD contain individual DNA-recognition sequences (Treisman, Harris, and Desplan 1991; Czerny et al. 1999), which enable them to independently occupy some target genes and/or cooperatively work on the promoters of some other genes via helix-turn-helix (HTH) motifs (H. E. Xu et al. 1999; W. Xu et al. 1995). This feature lays the structural foundation for the robust ability of PAX6 to bind diverse target genes from different tissues. Interestingly, an alternative splicing isoform of *Pax6*, PAX6(5a), includes a short 14-aa peptide within PD, which alters its DNA-binding activity and engages distinct target genes for regulation (Epstein et al. 1994; Xie and Cvekl 2011). Although PAX6(5a) is not as abundant as the conical PAX6 in most tissues, the loss of PAX6(5a) leads to iris hypoplasia and irregular iris morphology (Nishimura 2002). Additionally, the maintenance of certain ratios of PAX6(5a) and PAX6 is important during the proper differentiation of mouse lens, retina, and iris (Davis et al. 2009; Duncan et al. 2000; Sanjaya et al. 2002). Taken together, distinct DNA-recognition sequences on HD, PD, and PD(5a), establish a large spectrum of target genes regulated by PAX6 in different tissues. The C-terminal 153aa residue TAD domain of PAX6 is rich in proline (P), serine (S) and threonine (T), also called PST domain. Transcription factors often recruit co-interacting proteins (CIP) to achieve regulation of transactivation activity. In Leiden Open Variation Database (LOVD) reports more than 100 types of clinical cases with various mutations of the TAD region of *Pax6*. These include deletions, premature termination, and missense mutations. Many of these mutations cause TAD truncations and consequently lead to *Pax6* dysfunction. Notably, these patients displayed similar eye disorders

as those with dysfunction mutation at the DNA-binding domain of *Pax6*, which confirms the essential role of TAD. Although the importance of the PAX6 DNA binding domains have been deeply analyzed in the existing literature, the molecular understanding of TAD regulation remains relatively low. This study sought to reveal novel information regarding TAD regulatory mechanisms upon post-translational phosphorylation.

Previous studies have found that the function of protein PAX6 could be affected by post-translational modification. Several types of post-translational modifications occur on PAX6, including sumoylation, ubiquitination, acetylation, and phosphorylation. Sumoylation can facilitate PAX6 p32 (a shorter PAX6 isoform which contains only HD and TAD) to upregulate the expression of target genes via elevating the DNA binding activity in human lens epithelial cells (Yan et al. 2010), whereas sumolyzed PAX6(5a) is subjected to destabilization in human corneal endothelial cells (Yu et al. 2020). Despite the important roles of sumoylation in PAX6 isoforms, this modification occurs on lysine (K) residues in the DNA binding domains and not in the TAD. Second, Trim11, a ring finger E3 ubiquitin ligase, can modulate the degradation of PAX6 protein via the ubiquitin proteasome system (UPS) during cortical neurogenesis. Furthermore, Trim11 inhibits the transcriptional activity of PAX6 (Tuoc and Stoykova 2008). Although early research reports that PAX6 TAD could physically interact with Trim11 *in vitro* (Cooper and Hanson 2005), no direct evidence exists regarding the correlation of TAD-Trim11 interaction and the repression of PAX6 transcriptional activity. Next, the glycosylated form of PAX6 with O-N-acetylglucosamine (GlcNAc) residue is found on PAX6 and PAX6(5a) in the quail retina, while the glycosylation sites are mainly localized on its DNA-binding domains not TAD (Lefebvre et al. 2002). In contrast, all seven phosphorylation sites of PAX6 are located in TAD, which is present in all isoforms of *Pax6*. Additionally, several luciferase reporter assays (Yan et al. 2007; Kim et al. 2006) provided evidence that the promoters of αB-crystallin and proglucagon (two target genes of PAX6) were robustly turned up by wildtype PAX6 in contrast to the groups of PAX6 carrying multiple phosphorylation-site mutation *in vitro*, implicating that transactivation ability of PAX6 was potently repressed without TAD phosphorylation. Overall, given the impact of phosphorylation on regulating the function of the PAX6 TAD, I chose to investigate phosphorylation among all types of PAX6 post-translational modifications.

The highly-conserved PAX6 TAD is phosphorylated by p38 mitogen-activated protein kinase (p38 MAP kinase) at five amino acid threonine (T) or serine (S) residues (T303, T304, T360, S361, and S398) (Mikkola et al. 1999) and the homeodomain-interacting protein kinase 2 (HIPK2) at three amino acid threonine (T) residues (T281, T304, and T373) (Yan et al. 2007; Kim et al. 2006). These same phosphorylation sites existed in PAX6 of humans, mice, and zebrafish. In Mikkola and his colleagues' work, a protein sequence alignment of the PAX6 TAD was initially performed on PAX6 from six species ranging from sea urchin to human and several T and S residues were highly conserved. Furthermore, secondary structure element prediction highlighted four putative phosphorylation sites, which were predicted to be exposed away from any secondary structures (α-helix, β-sheet, or turn) and prone to be phosphorylated by MAP kinases. To verify these interesting sites, experiments conducted using *in-vitro* phosphorylation and [$_{32}$P]orthophosphate autoradiography demonstrated that TAD (derived from cDNA of zebrafish *Pax6*) was phosphorylated by p38 at three sites. Substitution mutation into alanine (A) at these sites (T303A/T304A, T360A/S361A, and S398A) could be phosphorylated due to loss of hydroxy group at the side chains. Phosphorylation by p38 on three-site-mutated PAX6 was proved to be

completely missing in contrast to the strong phosphorylation band of wildtype PAX6. Since these three "sites" involve five single amino acid residues, they are adjusted to five phosphorylation-sites (T303A, T304A, T360A, S361A, and S398A) for better clearance here. Besides, PAX6 TAD (encoded by a mouse embryonic cDNA) was found to be phosphorylated by HIPK2 as well (Kim et al. 2006). Co-immunoprecipitation (Co-IP) assays have demonstrated that PAX6 had a high affinity for HIPK2, and it was only the TAD and not the DNA binding domain that can be phosphorylated *in-vitro* by HIPK2. Additionally, three phosphorylation sites (T281, T304, and T373) on TAD were identified through Liquid chromatography-matrix-assisted laser desorption/ionization mass spectrometry (LC-MALDI-MS/MS), which used a tandem time-of-flight mass spectrometer. Taken together, there are seven phosphorylation sites (T281, T303, T304, T360, S361, T373 and S398) on TAD catalyzed by p38 and HIPK2. In this work, these sites were called by order as Site 1, Site 2, Site 3, Site 4, Site 5, Site 6, and Site 7 for short (see Fig. 2).

As mentioned above, TAD phosphorylation is able to strongly regulate the transcriptional capacity of PAX6. First, in HeLa and NIH 3T3 cells, co-transfection was performed with pG5E1bTATA-LUC reporter construct (harboring five copies of GAL4 binding sites(G5), E1bTATA promoter (Lillie and Green 1989) and luciferase gene) together with the construct containing the GAL4 DNA binding domain and wildtype PAX6 TAD or phosphorylation-site mutated TAD. Subsequently, the relative level of transactivation was determined. Loss of PAX6 TAD phosphorylation sites corresponded with a large reduction of transactivation in these assays. Notably, the loss of phosphorylation of site S398, site 7, had the greatest impact on PAX6 transactivation capacity among five single phosphorylation sites catalyzed by p38 (Mikkola et al. 1999). Interestingly, the five-site mutation led to a greater PAX6 transactivation capacity than that of Site-398 mutation, suggesting the presence of other phosphorylation sites on TAD. In addition, a similar luciferase system was applied to determine the sites on TAD by HIPK2 (Kim et al. 2006). A G5-TK-Luciferase reporter plasmid (containing G5 and the luciferase gene driven by a thymidine kinase minimal promoter), was co-transfected with plasmids encoding GAL4-PAX6 TAD and HIPK2 into the U2OS cell line. The relative transactivation of wildtype TAD was substantially greater than cells co-transfected with GAL4-PAX6 carrying mutation of three HIPK2-dependent sites. Overall, the p38 phosphorylation-sites and the HIPK2 phosphorylation-sites were independently determined to be crucial in modulating the transcriptional activity of PAX6. Nevertheless, all these sites have never been investigated together and a full analysis of the phosphorylation of all seven sites for the proper function of PAX6 is lacking. Besides, as above, phosphorylation of site S398 possesses more capacity in regulating PAX6 transactivation than the rest of other four single sites phosphorylated by p38. However, it remains unknown if site S398 is relatively more important compared to HIPK2 phosphorylation-sites. Therefore, I sought to answer these questions in the first part of this study by establishing an evaluation of the impact of all seven individual phosphorylation sites on the PAX6 transactivation domain.

TAD phosphorylation and PAX6 trans-repression ability

Besides to promote the expression of some target genes, PAX6 is also able to inhibit some other downstream gene expression. For instance, PAX6 can directly activate the expression of *Sfrp1*, *Sfrp2*, and *Dkk1*, which subsequently repress the canonical Wnt/β-catenin signaling in the lens surface ectoderm (Machon et al. 2009). In absence of *Pax6*, Co-IP assays found that these Wnt

inhibitors, SFRP1 and SFRP2, were profoundly reduced, leading to subsequent ectopic activation of Wnt signaling and disruption of normal lens development. Likewise, transcriptional repression by PAX6 also plays critical roles in embryonic development. Recently, bioinformatics analysis and functional studies have demonstrated that the gene *Mab21l2* is directly negatively regulated by PAX6 in mouse lenses (Wolf et al. 2009). In humans, the dysfunction of *Mab21l2* triggers bilateral iris coloboma with microcornea and corectopia as well as chorioretinal coloboma (Deml et al. 2015). Loss of *Mab21l2* causes the murine embryo to die at E12 with underdeveloped retinas (Wong and Chow 2002). In zebrafish, homozygous *Mab21l2* null mutants displayed severe lens and retina defects with embryo lethality (Deml et al. 2015). *Mab21l2* expression initiates at E8.5 in murine optic tissue, midbrain, branchial arches and forelimb bud, and its expression gradually ceases by E14. During eye development, MAB21L2 is very low in lens but abundant in optic vesicles. Nevertheless, the mRNA level of *Mab21l2* was significantly elevated in *Pax6*+/- lenses in comparison with wildtype lens tissue. Besides, based on the fact of high abundance of *Pax6* and low level of *Mab21l2*, it shows that a robust inhibition of *Mab21l2* from *Pax6* exists in lens epithelial development. Another target gene, Cone-Rod Homeobox (*Crx*), normally expressed in the peripheral RPCs of the optic cup, is directly down-regulated by PAX6 at E12 (Oron-Karni et al. 2008). Misexpression of *Pax6*, via *in vivo* injection and then electroporation in developing mouse eyes, resulted in the reduction of *Crx* expression and disruption of rod photoreceptor differentiation. Furthermore, co-introduction of *Pax6* and *Crx* rescues phenotypes caused by *Pax6* misexpression in photoreceptor precursors (Furukawa, Morrow, and Cepko 1997; Chen et al. 1997; Remez et al. 2017). Therefore, the proper inhibition of *Crx* by *Pax6* is essential in murine retinal development. There are also many genes negatively regulated by PAX6 in other tissues (for example, the brain and pancreas) and this PAX6 mediated repression is essential for proper tissue formation. In the embryonic cerebral cortex, *Foxd1* and *Isl1* were found to be directly repressed by *Pax6* through chromatin immunoprecipitation (ChIP) array along with expression analysis of *Pax6* gain and loss-of-function cortices. By downregulating the expression of the vital transcription factors, *Foxd1* and *Isl1*, *Pax6* could inhibit the neocortical identity of interneuron (Sansom et al. 2009). In the pancreas, PAX6 acts as a transcriptional repressor of many genes. For example, the PAX6 target gene *Ghrelin* is significantly upregulated in human and mouse β cells with deletion of *Pax6* (Alan W. Hart et al. 2013). Indeed, many genes have been recently found to be directly repressed by PAX6 in mammals, including *Pax2* (Bäumer et al. 2003; Schwarz et al. 2000), *Csf1* (Sun et al. 2016), *Snca* (Xie et al. 2013), cyclin D1 (Sun et al. 2015), γF-Crystallin in developing eyes (Yang et al. 2004), *Ascl1*, *Fezf2* in embryonic forebrain (Sun et al. 2015), glucagon, somatostatin, *Isl1*, and *Foxa2* in β cells of the pancreatic islets (Swisa et al. 2017). Taken together, the transcriptional repression of PAX6 is essential for the proper development of eyes, brain, and pancreas in humans and mice.

The existing data in *Drosophila* have suggested that the transcriptional repression of PAX6 is achieved through the interaction of its TAD with Gro, a co-repressor protein (Choi et al. 2005). In parallel, it has been demonstrated that TAD phosphorylation is able to strengthen the affinity of PAX6 to co-interacting proteins (like p300) when upregulating the expression of target genes (Kim et al. 2006). Hence, phosphorylation on TAD is highly likely to affect *Pax6*'s trans-repressive capacity on downstream genes. However, there is no knowledge available in any context regarding the correlation between TAD phosphorylation and transcriptional repression of PAX6. In the present study, I addressed this problem by determining the change of repressive target gene levels between the wildtype *Pax6* group and the phosphorylation-site-mutated *Pax6* group. This work

provides novel insights into the role of TAD phosphorylation in transcriptional repression of PAX6.

P*ax6* phosphorylation-site-mutated transgenic mice and mouse Pax6 null lens epithelial cell

Although the eye phenotype of Pax6 null transgenic mice is well known, there is little knowledge of the phenotype and developmental role of PAX6 TAD phosphorylation. To date, there have been several morphological studies of only HIPK2 and p38 MAPK, the two kinases that determine the phosphorylation-status of the PAX6 TAD. First, *Hipk2* has been characterized to be important for eye development. Deficiency of *Hipk2* in mice leads to small eyes with underdeveloped lens and cataract at an early age (Inoue et al. 2010). p38 MAPK is an essential gene for embryonic placental and vascular development (Cuenda and Rousseau 2007). A recent study demonstrated that inactivation of p38 protein is able to alleviate elevated intraocular pressure of glaucoma in adult mice, rats, and even squirrel monkeys (Lambert et al. 2020). Thus, these findings suggest that phosphorylation by HIPK2 and p38 MAPK plays a critical role in embryogenesis and maintenance of normal ocular environment. Therefore, HIPK2 and p38 work as multi-function factors in multiple tissues. However, direct evidence of the effect of PAX6 TAD phosphorylation by these kinases during mammalian eye development is lacking.

In addition to the *in-vitro* investigation of PAX6 TAD phosphorylation effect, I further explored if TAD phosphorylation is essential to murine eye development by generating a transgenic mouse line with mutation of *Pax6* phosphorylation-sites via the Clustered Regularly Interspaced Short Palindromic Repeats (CRISPR)/Cas9 genome editing tool (Ran, Hsu, Wright, et al. 2013). Since seven PAX6 phosphorylation-sites are scattered across about 3.5 kilo base pair(bp) of the mouse genome, it was difficult to create this type of transgenic mouse without antibiotic screening. Alternatively, with the use of ES (embryonic stem cells), it is possible to combine gene targeting with positive neomycin selection screening. Despite much effort, my experiments were not able to evaluate the role of each phosphorylation site on PAX6 in mouse eye development. However, we were able to confirm that phosphorylation of sites 2 and 3 on PAX6 are not required for normal eye development in mice.

Objectives/Goals

My *primary objective* was to determine the function and importance of mammalian PAX6 TAD phosphorylation *in vitro* and *in vivo*. My *central hypothesis* is that the dual function of *Pax6* as a trans-activator and trans-repressor is regulated by PAX6 TAD phosphorylation and plays a critical role in murine eye development. In Figure 3, the transactivation ability of PAX6 with all the seven phosphorylation-site mutation was analyzed *in vitro*. Based on the changes of reporter gene levels, PAX6 nearly lost all the transcriptional activity when all seven sites were mutated to the unphosphorylatable amino acid, alanine. Furthermore, phosphorylation of site 7 accounts for about 40% of the transcriptional activity, which plays the most dominant role among all the single phosphorylation-sites. Specifically, the downregulation of target genes by PAX6 was remarkably disrupted upon the mutations of *Pax6* phosphorylation sites. Thus, these *in-vitro* data demonstrate that PAX6 TAD phosphorylation is able to strongly affect the dual function of Pax6 as a trans-activator and trans-repressor. As to the transgenic mouse line with *Pax6* phosphorylation-site

mutations, I obtained a transgenic mouse line with mutations at both sites 2 and 3. These mice display normal eyes throughout the embryogenesis and postnatal development. This result showed that the phosphorylation on these two sites was not essential in modulating the transcriptional activity of *Pax6*, which is consistent with our *in-vitro* data. Unfortunately, no other transmittable phosphorylation-site mutations in transgenic mice were generated even though multiple approaches were employed. Additionally, a relatively simple system, the mouse lens epithelial cell line 21EM15, was employed to study the role of PAX6 TAD phosphorylation due to its unique potential that it can spontaneously form lentoid bodies (LB) during culture. I also established several *Pax6*-deletion cell lines (including Line F9 and B7). Nevertheless, none of them show any impact on the formation of LB, suggesting that *Pax6* is not essential for lentoid body formation.

Method and Materials

Constructs with single mutations of all seven sites via site-mutagenesis

To compare the importance of all sites during modulating TAD transcriptional activation, a series of constructs with single or multiple phosphorylatable serines (S) or theronines (T) mutated into alanines (A) were created by site directed mutagenesis. Primers (Integrated DNA Technologies IDT) used to create these constructs are listed in Table 1. Briefly, the plasmid pMXs-Pax6 (Addgene) with a wildtype Pax6 cDNA was mutated by PCR using the QuickChange Lightning Site-Directed Mutagenesis Kit (Agilent Technologies). This reaction was primed by a pair of primers with specific mutations at the 5' end and a desired mutant plasmid was generated with the rest of non-mutated circular DNA as templates using Q5 high-fidelity DNA polymerase (NEB). Plasmids carrying the desired mutations were selected and exclusively amplified prior to confirmation by sequencing assays (Eurofins Genomics) in Table 2. Another powerful kit, QuickChange Lightning Multi Site-Directed Mutagenesis Kit, facilitated all seven sites to be mutated successfully in one step. Mutated plasmids were established with the primers designed at a specific website (https://www.agilent.com/store/primerDesignProgram.jsp) by following the protocol of the kit. Likewise, mutations of the constructs were verified by sequencing analysis.

Cells

The murine lens epithelial cell line, 21EM15, (Reddan et al. 1989) was grown in MEF media containing DMEM supplemented with 10% fetal bovine serum, 1% non-essential amino acids, and 1% antibiotic-antimycotic (Thermo Fisher). The mouse kidney cell line, MK4, was grown in the same media as above. The mouse embryonic stem cell line, G4, (George et al. 2007) was cultured in DMEM high glucose supplemented with 10% knock-out serum replacement, 1% sodium pyruvate, 1% antibiotic-antimycotic, 1% non-essential amino acids, and 0.1% beta-mercaptoethanol in the presence of feeder mouse embryonic fibroblast cells, while neomycin-resistant G4 clones were picked up into gelatin-coated plates instead of the feeder cell environment.

To grow LBs, about 100 wildtype or mutated 21EM15 cells (fully trypsinized for over 10 min at 37º C) were seeded into each well of 96-well plates and cultured at 37º C with MEF media, with the media changed once every three days. After 1 week, cells reached 80% confluency. Then cells were checked every day for fried-egg structures (some cells simultaneously aggregate to roughly

form a 2D circle with lower transparency as the central part of a fried egg) until the onset of lentoid body formation, and then the fresh media was changed once per 48 hours. After fried-egg clusters were formed, the media were replaced every 24 hours to generate mature LB with cells aggregating into a ball-like 3D structure.

Luciferase assay to determine the effect of phosphorylation site mutations on PAX6 transactivation

To evaluate the relative transactivation strength of all sites, MK4 cells with low endogenous abundance of PAX6, were grown in DMEM supplemented with 10% fetal bovine serum, 1% non-essential amino acids, and 1% antibiotic-antimycotic until confluency at which point, they were passaged twice. After reaching 80% confluence, the cells were transfected using Turbofect Transfection Reagent (ThermoFisher #R0531) with the appropriate vectors following the manufacturer's protocol. The vector DNA containing a PAX6-inducible promoter (Cignal Reporter, Promega 336841) and the mutated *Pax6* cDNA constructs (with phosphorylatable serines and/or threonines replaced with alanine(s)) were co-transfected into MK4 cells. After 32 hours, cells were collected and lysed to conduct Luciferase assays using the Dual-Luciferase Reporter Assay System (Promega E1910) according to the manufacturer's instructions, and the ratios of the luminescence intensity by firefly luciferase over the one by Renilla luciferase was measured on Luminometer (Nicar). Then, a comparative analysis was performed among all the mutant groups. ANOVA test was conducted as statistical analysis.

RT-qPCR assay

As previously described (Padula et al. 2019), total RNA was extracted from MK4 transfected cells via an RNA extraction kit (Zymo Research) and DNase I digestion was performed to eliminate DNA prior to reverse transcription of the isolated RNA (Promega ImProm-II™ Reverse Transcription). Concentrations of cDNA from amplified samples were analyzed through a Nanodrop Spectrophotometer. Real-time quantitative PCR was performed on a Bio-Rad CFX device to examine the level of specific gene expression via GoTaq Promega qPCR master mix (Promega). Intron-spanning primers were designed to specifically quantify targeted mRNA transcripts. Glyceraldehyde 3-phosphate dehydrogenase (Gapdh) expression was used as an endogenous control (sequences were listed in Table 3). The cycling conditions consisted of 1 cycle at 95 °C for 120 s for denaturation, followed by 40 two-step cycles for amplification (each cycle consisted of 95 °C incubation for 15 s and an appropriate annealing temperature as the annealing and product elongation temperature for 60 s). The reaction specificity was checked by the melting temperature and the presence of a single DNA band on agarose gels from the RT-qPCR products. The melting curve cycle (Cq) was generated from the RT-qPCR reaction, and gene expressions were calculated and normalized to GAPDH level using the delta-delta Ct method. ANOVA test was conducted as statistical analysis.

To examine the role of *Pax6* phosphorylation on transcriptional capacity in *Pax6* null 21EM15 cells, pMXs-*Pax6* constructs were transfected via Turbofect Transfection Reagent and then total mRNA was isolated from cells after 36 hours to assess gene expression changes among interesting

target genes between the groups transfected with wildtype and phosphorylation-site mutated *Pax6* constructs.

Animals

All procedures were approved by the Miami University Institutional Animal Care and Use Committee and complied with the ARVO Statement for the Use of Animals in Research, consistent with those published by the Institute for Laboratory Animal Research (Guide for the Care and Use of Laboratory Animals). In the initial experiment, a strategy, double nicking by RNA-guided CRISPR Cas9, was utilized to increase specificity and minimize off-target cutting (Ran, Hsu, Lin, et al. 2013) in Fig. 3. In this research, all sgRNAs were designed using the software on the website (https://zlab.bio/guide-design-resources). Due to the size restriction of the single strand DNA template (ssDNA, 200 nt at maximum, Integrated DNA Technologies), the first three phosphorylation-sites were targeted to be mutated into A in one experiment, in which FVB/N zygotes were injected with the fresh TE buffer added with 20 μg/μL Cas9 Nickase mRNA, 20 μg/μL of a single guide RNA (sgRNA 1, Integrated DNA Technologies), 20 μg/μL of a second single guide RNA (sgRNA2, Integrated DNA Technologies), and 10 μg/μL of ssDNA template (Table 4). Following microinjection, zygotes were implanted into ICR host females, and resultant pups were collected for genotyping and phenotyping analysis to investigate the role of PAX6 phosphorylation during eye development (Fig. 4). In genotyping analysis, PCR assays were conducted based on Fig. 5B. Finally, sequencing analysis were conducted on single DNA copies containing site 1, 2, and 3 via subcloning (PCR cloning kit, Promega corporation). Alternatively, successful genome editing created a restriction site that could be cleaved by the enzyme, *MluCI* (NEB), creating a cheaper and faster method for screening than direct sequencing assays.

In parallel, I attempted to create the transgenic mice with all phosphorylation-site mutations using CRISPR/Cas9 with double sgRNAs. I devised a method to target all seven sites simultaneously. Wild type mouse zygotes were introduced with a mixture of Cas9 enzyme, sgRNA 1, sgRNA 5, and a double-strand homologous repair DNA template containing desired mutations via microinjection (Table 5), so that a DNA fragment between the two cleavage sites was cut out by Cas9 enzyme guided by two sgRNAs. This design facilitated the repair of the broken genomic DNA via homology-directed repair (HDR) using the DNA template carrying the mutations in all seven sites (Fig. 6). Next, as Fig. 5 and Table 5 showed, the same strategy as above was conducted in the first part of genotyping of these mice, including digestion by the restriction enzyme, *MluCI* (NEB), and then sequencing analysis. To further identify whether seven phosphorylation-sites of the mice were mutated, genomic PCR was conducted for DNA copies for sequencing. Firstly, to ensure the tested DNA located on the expected position, one of the primers was designed to bind to the upstream DNA of 5'HA (Homology Arm) and the reverse primer targeting the downstream DNA of Site 3. Then, with the PCR product as the template, the DNA copies with a size of about 0.5kb, were acquired in the second PCR for sequencing, which was covered by one read.

Another strategy was to create transgenic embryos with all phosphorylation-site mutation *Pax6* derived from mouse embryonic stem cell G4. In this way, mouse stem cells would be manipulated instead of mouse zygotes to permit positive selection with the neomycin drug, G418 disulfate salt (Sigma-Aldrich) to increase the rate of stem cells with desired mutations out of thousands of total cells. With the microinjection method it's less likely to obtain the desired mutations in zygotes

without any selection because of the low efficiency of long DNA editing. Initially, the preliminary experiment was conducted to identify the optimal sgRNA pair responsible for all-site mutation of *Pax6* in the MK4 cell line. Cells with the desired mutations would exhibit the resistance to G418 (Fig. 7, Table 6). In the cells targeted with sgRNA2 and 4, 12 colonies were acquired in the media containing 700 ng/uL of neomycin after 10 days of selection, and genotyping analysis found that all seven sites of *Pax6* in these MK4 cells were mutated properly. However, no cells survived under the neomycin environment in the cells targeted withsgRNA1 and 5 or cells from the control group. Therefore, sgRNA2 and 4 was chosen to make the seven-site mutants using embryonic stem cells. As shown in Fig.8, a pair of single gRNAs (one sgRNA targeting the relative 5' side of the mutated DNA region, and another sgRNA at the 3' end) were inserted in the plasmid, px458 (Addgene) containing Cas9 DNA, separately. Additionally, a DNA fragment that included sites 1-7 (about 3.7kb in size) flanked with 0.8 kb DNA at each end as homology arms was cloned into a plasmid, pMINI-T, via a PCR cloning Kit (NEB). As repair template, multiple-site mutations from T or S into A plus missense mutations of the PAM sites were introduced into the pMINI-T construct via QuickChange Lightning Multi Site-Directed Mutagenesis Kit. To facilitate selection for mutated cells, a neomycin-resistance gene driven by an independent phosphoglycerate kinase (PGK) promoter was inserted into the middle of intron 10. After the confirmation by sequencing analysis, three types of constructs (two sgRNA constructs and one repair template construct) were co-transfected into G4 cell line via electroporation (Bio-Rad Gene Pulser Xcell modular electroporation systems). Then, the drug, G418, was applied from 100 μg/mL and slowly increased to 250 μg/mL to poison cells without the neomycin-resistant gene. Finally, the surviving cells were grown into single clones. Half of each single clone was used for genotyping analysis. To amplify the edited region, at least one primer was directed to the DNA region located outside of repair template sequence, eliminating the possibility of mis-insertion of template into non-*Pax6* region on genome. Two long DNA fragments (one containing Site 1, 2, and 3; another site 4 to 7) were acquired by following the strategy shown in Figure 5. Instead of sequencing these long DNAs from all the Neo-resistant clones directly, an additional round of PCR was performed to generate three shorter DNA fragments containing sites 1-3, Site 4-6, and Site 7, separately. As shown in Fig.5, two novel restriction sites, *MluCI* and *BsrDI* (NEB) were introduced during the mutation of *Pax6* and these are unique within the shorter DNA sequences (0.5 or 0.6 kb in size). Therefore, only DNA fragments that could be cut by *MluCI* and *BsrDI* were selected for further sequencing assays to confirm the presence of all seven phosphorylation-site mutations.

G4 clones (feeder-cell free) with proper mutations at all sites were intended for generating transgenic mouse lines. Wildtype ICR blastocysts were collected at E3.5 and then injected with targeted G4 ES cells. Next, chimeric blastocysts were transferred into pseudo-pregnant ICR females to generate live chimeric animals that were distinguished by coat color. ICR mice are albino, but the G4 ES cells are agouti. Chimeric mice were mated to normal FVB/N adults to transmit the mutant *Pax6* allele through the germline. Additionally, since G4 cells harbor XY chromosomes and agouti coat alleles, male chimeric mice with more brown color coat were able to exhibit stronger potential to transmit mutations to offspring by mating with FVB/N female mice (see Fig. 8).

Western Blot and Histological analysis

Briefly, cell pellets were collected from MK4 or 21EM15 cells transfected with *Pax6* constructs and then washed with cold PBS buffer carefully twice. Next, RIPA lysis buffer (ThermoFisher Scientific) was added to re-suspend the pellets and mixed thoroughly via gently shaking for 15 min on ice. The mixture was centrifuged at ~14,000 × g for 15 minutes, and the supernatant would be kept as total protein extracted from lysed cells. After quantification analysis using the Pierce BCA Protein Assay Kit (ThermoFisher Scientific 23225), 20 μg of protein samples was boiled for 5 minutes in 4X Laemmli sample buffer (Bio-Rad) supplemented with β-Mercaptoethanol and then loaded into single wells of 12% SDS-PAGE (sodium dodecyl sulphate–polyacrylamide gel electrophoresis) gel, separately. After electrophoresis for 1.5h in Bio-Rad Running reagent at a voltage of 200mV, proteins were then transferred onto PVDF membrane using the Bio-Rad TurboBlot system. Blots were blocked in 5% BSA in tris buffered saline with 0.1% Tween-20 (TBST) and incubated in the primary antibody overnight at 4° C. The following primary anti-PAX6 antibodies (Santa Cruz, sc-81649) were used at 1:200 dilution. Primary antibody was detected using the secondary goat anti-mouse antibody (Bio-Rad 12005867) and imaged using the Bio-Rad ChemiDoc Touch Imaging System.

New-born embryos were collected and fixed in 10% neutral buffered formalin overnight at room temperature. Standard protocols (Titford 2009; Hoang et al. 2017) were used to fix and embed tissue in paraffin wax before embryos were sectioned at 5μm. Sections were subjected to xylene washes followed by dehydration. For histological analysis, standard Hematoxylin and Eosin staining protocols were used and lens sections were imaged on a Nikon TI-80 microscope.

Mouse lens epithelial cell line with *Pax6* mutation

As an alternative to transgenic mice, the mouse lens epithelial cell line, 21EM15, was employed to study the role of the PAX6 TAD phosphorylation, based on its unique potential to spontaneously form LB during culture. Similar genome-editing materials (the ones to create ES-derived transgenic mice) were used to create a *Pax6* phosphorylation-site mutation cell line when 80% confluence cells were co-transfected via Turbofect Transfection Reagent. In the meantime, to test if *Pax6* is required for LB formation, *Pax6*-null 21EM15 cells were generated in combination with the construct px458 inserted with sgRNA8 (see Table 7), in which a cleavage would occur around the transcription starting site of *Pax6* combined with non-homologous end joining (NHEJ) repair to create indel frameshift mutations. Then, single cells were seeded into individual wells on 96-well plates and cultured to form clonal colonies. Unlike the genotyping strategy above to detect missense mutations, genome PCR was conducted on single clones to screen for indels generated at the cleavage site region targeted by sgRNA8 in contrast to the DNA size of wildtype cells, and then single cDNA copies of the clones with indel mutation were prepared for sequencing analysis. Thus, interesting clones were confirmed at DNA level. Next, PAX6 protein in these clones were further examined through Western blot to verify the absence of PAX6 compared to the wildtype PAX6 from control 21EM15 cells.

Results and Discussion

Evaluation of all seven phosphorylation-sites of *Pax6* TAD

The relative transactivation capacity of PAX6 with all seven phosphorylation-sites mutated into alanine was only 20% that of that from cells transfected with wild-type PAX6 (Fig. 9), implying a remarkably reduction of transactivation capacity of PAX6 due to loss of TAD phosphorylation. This was similar to the activation of the PAX6 luciferase reporter in the negative control (GFP) transfected cells, in which no PAX6 was expressed. This finding demonstrated that the ablation of phosphorylation modification on PAX6 led to a complete depletion of the transcriptional activation capacity of *Pax6*, suggesting that phosphorylation of TAD is essential for maintaining the transactivation ability.

Among all the single or double phosphorylation-sites in this assay, site 7 was characterized as the most important site. As shown in Fig. 9, loss of phosphorylation at site 7 reduced the relative transactivation capacity by approximately 30% and this was the greatest effect for any single site mutation. Other single or double phosphorylation-site mutations, without the inclusion of site 7, made little difference in the transactivation capacity of PAX6. Although the role of site 7 (the corresponding conserved site in zebrafish) had been noted earlier among five p38-catalyzed sites in zebrafish (Mikkola et al. 1999), in which Site 7 exhibited greater importance than other single p38-catalyzed sites, this work provided a comprehensive understanding of the great importance of Site 7 among all seven phosphorylation-sites in mice. Taken together, these results demonstrate that mutating all the phosphorylation sites on *Pax6* results in an effect similar to the *Pax6* null mutation and mutating Site 7 alone should cause a hypomorphic mutation in mice.

Pax6's trans-repression capacity was strictly tuned by TAD phosphorylation

As a dual role factor, PAX6 was also examined to determine whether the phosphorylation modification of TAD would affect the ability of PAX6 to repress transcription. Wildtype *Pax6* and the phosphorylation-site mutation *Pax6* constructs were transfected into MK4 cells, respectively, and then downstream target genes, previously shown to be repressed by PAX6 in literature, were examined for their expression changes between the groups of various transfectants with GFP and *Pax6* constructs. As shown in Fig. 10A, overexpression of wildtype *Pax6* and the phosphorylation-site mutated *Pax6* constructs were successful, in which the mRNA levels of *Pax6* transcribed by three *Pax6* constructs were significantly higher than that of cells transfected with GFP construct. The two mutated *Pax6* constructs displayed even more transcripts than the wildtype *Pax6* construct, though all groups were treated with the same amount of plasmid. Moreover, the protein levels of *Pax6* in all four groups were determined by Western blot assay (Fig. 10B), and the result was remarkably consistent with the data in Fig. 10A. Due to the poor abundance of endogenous

Pax6 in MK4 cells, minimum levels of *Pax6* mRNA and protein were detected in cells transfected with GFP construct. In other three groups, wildtype and mutated PAX6 were strongly translated by *Pax6* constructs, and wildtype PAX6 exhibited a weaker band than that of two mutated PAX6, which also confirmed the RT-qPCR data in Fig. 10A. These outcomes demonstrated that the treatment of introducing exogenous PAX6 to MK4 cells was effective.

In Figure 11, the expression of two repressive target genes, *Csf1* (Sun et al. 2016) and *Pax2* (Schwarz et al. 2000), was reduced by 60% and 50%, respectively when transfected with wildtype *Pax6* relative to their expression when transfected with GFP. However, the introduction of all seven phosphorylation-site mutated PAX6 failed to significantly reduce either *Csf1* or *Pax2* expression, implying the complete inactivation of *Pax6* phosphorylation at seven sites abolished the inhibition of the expression of *Csf1* and *Pax2*. Additionally, based on the comparative analysis of the Just-Site-7 group, the wildtype group and the GFP group, the levels of *Csf1* and *Pax2* in the Just-Site-7 group were greatly elevated from these in wildtype group, while they were still significantly lower than those in the GFP group. These results indicated that the inactivation of only Site 7 was able to partially rescue the expression of both genes. Furthermore, the levels of *Pax2* and *Csf1* in the Just-Site-7 group was significantly restored to about 80% of that of the all-phosphorylation-site group, suggests that phosphorylation at site 7 exhibited a greater importance in modulating the repression by PAX6 than that of PAX6 activation.

In addition, the relative level of *Pax6* in the wildtype group was only 3, which was much lower than 7 or 8 in the Just-Site-7 group and the all-phosphorylation-site group, respectively. Of note, the relative expression of both *Csf1* and *Pax2* in the wildtype group was just 0.4 in contrast to 1 of the other two *Pax6* mutant groups (see Fig. 11). Taken together, a relatively low level of PAX in wildtype construct group still could remarkably inhibit the expression of both gene, whereas the relative high levels of PAX6 in two mutated construct groups failed to maintain the transcription repression due to phosphorylation-site mutation at PAX6 TAD. These results demonstrated that the repression of *Pax6* on target gene expressions was remarkably attenuated by TAD phosphorylation. Overall, I concluded that the trans-repression ability of *Pax6* was potently regulated by TAD phosphorylation.

The molecular mechanism of how target gene expression is activated or inhibited by PAX6 remains to be illustrated. The existing data found that PAX6 acts by forming a complex, including additional DNA-binding factors and co-interacting factors associated with core histone posttranslational modifications (PTMs). Jian Sun and his colleagues raised a model (Sun et al. 2016), in which PAX6, accompanied with *Sox2, Maf* and *Set1a*, can recruit Mll1/2 complexes and p300 to promote the transcriptions. Besides, to repress downstream gene transcription, it indicates that PAX6 needs to interact with Groucho (co-repressor), and HDAC in Drosophila (Choi et al. 2005). Therefore, PAX6's regulatory complexes require co-DNA-binding factors and co-interacting factors, leading to loss or gain histone methylation or acetylation at PAX6-binding DNA areas.

Pax6 phosphorylation-site mutated transgenic mice

Since Site 1, 2, and 3 are closer than the rest of the four sites in the location of the genome, the first three sites were initially designed to be mutated into A in the one experiment via

CRISPR/Cas9 nickase technique (Ran, Hsu, Lin, et al. 2013). FVB/N wildtype zygotes were introduced with sgRNA1, sgRNA2, single strand DNA template ssDNA, and 20 μg/μL Cas9 nickase mRNA via micro-injection, and then these zygotes were implanted into ICR host females. In this experiment, one founder mouse (ID: 1280) heterozygous for mutations of T303A (site 2) and T304A (site 3) was obtained through double nicking CRISPR/Cas9 system via zygote microinjection (Fig. 12A and B). To get the homozygous mutants, 1280 was mated with FVB/N wildtype mice and then the offspring were intercrossed. These homozygotes appeared normal with respect to eye development (Fig.12C and D). Thus, it indicated the phosphorylation of these two sites were dispensable to proper eye formation and the other five sites were still sufficient to activate PAX6. This outcome was consistent with the result of luciferase assay above that no significant differences were observed in the activation ability of *Pax6* in the group of Site 2 and 3 mutated (see Fig 9, site 2 + 3 A).

A second transgenic founder female mouse (ID: 1270) was acquired along 1280, and all 4 single DNA copies via subcloning from the product of genome PCR were sequenced to be mutated at three phosphorylation-sites. It proved that at least the tail tissues of 1270 that were used for genotyping contained desired mutations at both alleles. Although it carried the wanted mutation at Site 1, 2, and 3, it displayed normal eyes and was unable to transmit the mutated *Pax6* to its offspring based on the fact that over 40 pups were screened to be wildtype mice without any *Pax6* phosphorylation-site mutation. This phenomenon could be interpreted that CRISPR/Cas9 materials started to work at a later embryogenesis stage of 1270 rather than single-cell zygote stage so that part of the multi-cell embryo was not subject to genome editing and the rest was mutated by CRISPR/Cas9 materials. Consequently, 1270 developed into a mosaic mouse and its germinative cells were unmutated in *Pax6*. Thus, this line could not serve as a good model for this study.

To accelerate the study of the role of TAD phosphorylation in murine embryogenesis, I switched to create transgenic mice targeting all seven phosphorylation-sites directly in one experiment. To mutate all phosphorylation-sites on *Pax6*, a donor DNA was constructed carrying seven alanine mutations on the corresponding sites flanked by a repair arm with 0.8 kb in size at each end. Only 5 wildtype mice were obtained after two rounds of zygote microinjection based on CRISPR/Cas9 technique. I also used mouse embryonic stem cells that were manipulated by the CRISPR/Cas9 genome editing tool. The donor DNA was inserted with a neomycin-resistance gene, which could facilitate the screening for the mutated cells. Although about 65 single colonies gained the resistance to G418, the genotyping assays showed that the neomycin-resistance gene was not integrated into *Pax6* in any of these colonies. We assumed that the gRNA didn't work well, and thus it failed to initialize the homology repair on the *Pax6* gene. Therefore, I was unable to generate mice having phosphorylation site mutations as sites other than 2 and 3.

To select new sgRNA pairs, another preliminary experiment was conducted in MK4 cells, which grew more quickly in a cheaper media than the G4 ES cells. The new sgRNAs with higher efficiency would establish more cell clones with the neomycin resistance. Cells targeted with sgRNA2 and sgRNA4 (Table 6) were found to develop the most neomycin-resistant clone plate after 10 days of positive selection. Further genotyping analysis of these clones revealed that all seven phosphorylation sites were mutated properly. Conversely, no clones survived under the neomycin environment in the group of sgRNA1 and sgRNA5, indicating poor performance by this pair of sgRNAs. Therefore, sgRNA2 and 4 were chosen to target another batch of ES cells.

Subsequently, I acquired Clone 67, which was hemizygous in Site 1, 2, and 3 but homozygous in Site 4-7, meaning that the seven sites of *Pax6* on one allele were completely mutated as desired whereas Site 1-3 still unmutated on *Pax6* of another allele in Clone 67. This was the best clone among over one hundred clones that I tested. Clone 67 was injected into wildtype blastocyst embryos to obtain chimeric offspring. These chimeric mice were mated with normal FVB/N mice in an attempt to achieve germline transmission and to acquire *Pax6* phosphorylation-site mutation animals. In Fig.13, 4 Clone-67-derived chimeric mice (3 females and 1 male) were obtained with normal eyes, but they were either infertile or unable to transmit the G4 mutations to the next generation. Interestingly, all the three female chimeric mice displayed dramatically larger coat areas in black than that of the male. Among the mice, one female with the largest black coat area (up to 70% of the total area) was infertile, suggesting that its cells in the reproductive system originated from G4 stem cells containing X and Y chromosomes.

These results indicated the double-sgRNA genome-editing strategy is not friendly to create *Pax6* mutant mice. There are two possibilities for why no *Pax6* mutated mice were available. First, my CRISPR/Cas9 system worked poorly and failed to edit *Pax6*. Apparently, it is rejected by the fact that I have got *Pax6* mutated cell lines of both MK4 cells and G4 cells. Another possibility is that *Pax6* was over-edited in double-sgRNA strategy, leading to a serious impairment or even failure of normal murine embryogenesis. It implies that double or single cleavages were introduced well to *Pax6*, but it wasn't repaired or mis-repaired on the genome. Consequently, the embryos with the dysfunction of Pax6 were unable to develop successfully. To date, all the data is prior to support this possibility. Besides, since NHEJ occurs more frequently than HDR to repair the broken genomic DNA in CRISPR/Cas9 system, it's very likely to form a mutant cell/mouse with one allele repaired through HDR carrying the neomycin resistant gene and the other allele via NHEJ. In this case, the function of *Pax6* on both alleles was abolished and thus it led to the mal-development or under-development of mice, making it nearly impossible to get live newly born animals. Transgenic mice served as the platform in the entire research, but this process is overwhelmingly inefficient. Apparently, it's necessary to propose an alternative since no satisfying transgenic mice were established after five years. To replace transgenic mice, 21EM15 cells were manipulated to be edited on genomic *Pax6* through CRISPR/Cas9 technique, in which more cell materials could be collected efficiently for cell screening and clone genotyping. In addition, 21EM15 cells can spontaneously grow LB, and the role of phosphorylation of PAX6 TAD was determined during this process.

Pax6-null mouse lens epithelial 21EM15 cell line

The CRISPR/CAS9 technique with sgRNA8 was utilized to knockout *Pax6* from 21EM15 cells by introducing a cleavage site within the second coding exon (exon 4), which was very close to the transcription starting site of *Pax6* depicted in Fig. 14 and Table 7. Technically, after sgRNA8-px458 including the Cas9-coding region was transfected into 21EM15 cells, CAS9 protein and sgRNA8 were expressed in transfected cells and an indel mutation on *Pax6* was created by NHEJ to repair the CAS9-induced double strand DNA break. Hence, three mutated clones, F9, D8, and B7, were created and their genotype information were listed in Table 8. First, one in-frame mutation (36-bp deletion) in D8 still led to the production of a truncated PAX6 and it could not

destroy PAX6. Secondly, F9 was also found to contain an indel at the same spot as D8, whereas the protein PAX6 was abolished upon the frameshift mutation (44-bp deletion) in F9. As to B7, a largest indel (about 61bp deleted) was seen in Table 8, while the DNA copy (300bp approximately) were sequenced to be an irrelevant DNA fragment which was about 60bp shorter than that of wildtype DNA. Hence, D8 was eliminated from the following studies, and F9 and B7 were further investigated via WB. As shown in Figure 15, PAX6 protein was ablated in F9 and B7. By the protocol of LB culturation, normal LBs were observed in F9 and B7, which were similar in size and shape to wildtype-cell-originated LB in Figure 16. Therefore, it proved that *Pax6* is not required for LB formation in 21EM15 cells.

Conclusions and Future Studies

In this study, PAX6 TAD phosphorylation is able to strongly affect the dual function of *Pax6* as a trans-activator and trans-repressor *in vitro*. First, the transactivation ability of seven phosphorylation-sites on PAX6 TAD was compared in one experiment *in vitro* for the first time. PAX6 nearly lost all the transcriptional activity when phosphorylation at all seven sites were abolished. Moreover, phosphorylation of site 7 (S398 in mice) accounts for about 40% of the transcriptional activity and plays the most dominant role among all the single phosphorylation-sites. Additionally, in MK4 cells, the repression of target genes (*Pax2* and *Csf1*) by PAX6 was remarkably disrupted upon the complete dephosphorylation on PAX6 and the expressions of genes were promoted up to two folds compared to the group transfected with wildtype *Pax6*. Importantly, a largely rescued expression was observed in both target genes when Site 7 was specifically mutated. Overall, I concluded that the dual functions of *Pax6* as a trans-activator and trans-repressor were firmly tuned by phosphorylation modifications at seven sites of TAD, particularly Site 7.

However, one question that might challenges these results is that the dysfunction of mutated PAX6 is potentially caused by the mis-conformation due to mutation. To eliminate this possibility or to ensure that the changes in PAX6's transactivation/trans-repression capacities is resulted from its loss of TAD phosphorylation, a supplementary experiment will be performed by knocking down *Hipk2* and p38 in MK4 cells using small interfering RNAs (siRNA). Specific siRNAs will be applied to MK4 cells to silence the expression of *Hipk2* and p38, and then same luciferase assay or RT-qPCR as above need to be conducted in these pre-treated cells. A negative result with no significant difference in all the groups transfected with wildtype or mutated *Pax6* constructs will demonstrate that the effects are caused by the alteration of TAD phosphorylation status. Nevertheless, if the same responses are observed as the results in MK4 cells without siRNA treatment, it will imply that phosphorylation-site mutation disrupts the normal confirmation of PAX6 protein and consequently destructs its function. Although there is no a certain answer to this question before the experiment is completed, I'm prior to assume that the mutation of phosphorylation sites will not lead to the alteration of PAX6' proper conformation, given to the outcome of normal eyes in transgenic mouse with site 2 and 3 mutations.

During several efforts of generating the transgenic mouse line with *Pax6* phosphorylation-site mutation, a transgenic mouse line with the mutation at Site 2 and 3 was acquired and displayed

normal eyes. To gain more *in vivo* evidence regarding the role of TAD phosphorylation in the murine eye development, mouse stem cells were manipulated via CRISPR/Cas9 technique and antibiotic screening was performed to increase the rate of clones with desired mutations. Thus, Clone 67 was obtained with seven *Pax6* phosphorylation-sites mutated on one allele and Site 4-7 mutation on another allele, whereas no C67-derived phosphorylation-site mutated mice were produced. Besides, a few partially mutated cell 21EM15 cell lines (including Clone 4 and Clone 25) and several *Pax6*-deficient cell lines (Clone F9, and B4) were acquired containing mutated Site 1,2, 3 and a following 75-bp deletion. Nevertheless, none of them show any impact on the formation of LB, suggesting that *Pax6* is not essential to this process. Although it has been revealed that the dual function of *Pax6* was strictly regulated by PAX6 TAD phosphorylation *in vitro*, the research of the function of *Pax6* TAD phosphorylation in the murine eye formation *in vivo* still remained elusive.

For future work, we could determine the molecular mechanism of how PAX6 trans-repressive ability is regulated by the phosphorylation state of PAX6 TAD *in vitro*. The existing evidence has demonstrated that the TAD phosphorylation could elevate the affinity of PAX6 to the co-interacting protein p300 to activate the transcription of target genes. During the process, p300 was characterized as a co-activator. However, there is little known about the co-repressors recruited by PAX6 to inhibit gene expression. Interestingly, a candidate, Groucho acting as a co-repressor, has been proved to be essential in eye development of *Drosophila* (Sekiya and Zaret 2007). Finally, the co-binder Groucho would be detected through Co-immunoprecipitation and western blot to illustrate if the interaction with PAX6 was affected by TAD phosphorylation in MK4 cells with the introduction of wildtype *Pax6* and phosphorylation-site mutated *Pax6*, respectively. Furthermore, mass spectrometry could be conducted to verify Groucho and further identify more novel co-binders.

Literature Cited

Adams, Julian. 2003. “The Proteasome: Structure, Function, and Role in the Cell.” *Cancer Treatment Reviews* 29 Suppl 1 (May): 3–9.

Ashery-Padan, R., T. Marquardt, X. Zhou, and P. Gruss. 2000. “Pax6 Activity in the Lens Primordium Is Required for Lens Formation and for Correct Placement of a Single Retina in the Eye.” *Genes & Development* 14 (21): 2701–11.

Ashery-Padan, Ruth, Xunlei Zhou, Till Marquardt, Pedro Herrera, Leanne Toube, Asher Berry, and Peter Gruss. 2004. “Conditional Inactivation of Pax6 in the Pancreas Causes Early Onset of Diabetes.” *Developmental Biology* 269 (2): 479–88.

Bäumer, Nicole, Till Marquardt, Anastassia Stoykova, Derek Spieler, Dieter Treichel, Ruth Ashery-Padan, and Peter Gruss. 2003. “Retinal Pigmented Epithelium Determination Requires the Redundant Activities of Pax2 and Pax6.” *Development* 130 (13): 2903–15.

Callaerts, P., G. Halder, and W. J. Gehring. 1997. “PAX-6 in Development and Evolution.” *Annual Review of Neuroscience* 20: 483–532.

Chen, S., Q. L. Wang, Z. Nie, H. Sun, G. Lennon, N. G. Copeland, D. J. Gilbert, N. A. Jenkins, and D. J. Zack.

1997. “Crx, a Novel Otx-like Paired-Homeodomain Protein, Binds to and Transactivates Photoreceptor Cell-Specific Genes.” *Neuron* 19 (5): 1017–30.

Choi, Cheol Yong, Young Ho Kim, Yong-Ou Kim, Sang Joon Park, Eun-A Kim, William Riemenschneider, Kathleen Gajewski, Robert A. Schulz, and Yongsok Kim. 2005. “Phosphorylation by the DHIPK2 Protein Kinase Modulates the Corepressor Activity of Groucho.” *The Journal of Biological Chemistry* 280 (22): 21427–36.

Cooper, Simon T., and Isabel M. Hanson. 2005. “A Screen for Proteins That Interact with PAX6: C-Terminal Mutations Disrupt Interaction with HOMER3, DNCL1 and TRIM11.” *BMC Genetics* 6 (August): 43.

Cuenda, Ana, and Simon Rousseau. 2007. “p38 MAP-Kinases Pathway Regulation, Function and Role in Human Diseases.” *Biochimica et Biophysica Acta (BBA) - Molecular Cell Research*. https://doi.org/10.1016/j.bbamcr.2007.03.010.

Cvekl, Aleš, and Ruth Ashery-Padan. 2014. “The Cellular and Molecular Mechanisms of Vertebrate Lens Development.” *Development* 141 (23): 4432–47.

Czerny, T., G. Halder, U. Kloter, A. Souabni, W. J. Gehring, and M. Busslinger. 1999. “Twin of Eyeless, a Second Pax-6 Gene of Drosophila, Acts Upstream of Eyeless in the Control of Eye Development.” *Molecular Cell* 3 (3): 297–307.

Davis, Noa, Chen Yoffe, Shaul Raviv, Ran Antes, Joachim Berger, Silvia Holzmann, Anastassia Stoykova, Paul A. Overbeek, Ernst R. Tamm, and Ruth Ashery-Padan. 2009. “Pax6 Dosage Requirements in Iris and Ciliary Body Differentiation.” *Developmental Biology* 333 (1): 132–42.

Deml, Brett, Ariana Kariminejad, Razieh H. R. Borujerdi, Sanaa Muheisen, Linda M. Reis, and Elena V. Semina. 2015. “Mutations in MAB21L2 Result in Ocular Coloboma, Microcornea and Cataracts.” *PLoS Genetics* 11 (2): e1005002.

Duncan, M. K., Z. Kozmik, K. Cveklova, J. Piatigorsky, and A. Cvekl. 2000. “Overexpression of PAX6(5a) in Lens Fiber Cells Results in Cataract and Upregulation of (alpha)5(beta)1 Integrin Expression.” *Journal of Cell Science*. https://doi.org/10.1242/jcs.113.18.3173.

Epstein, J. A., T. Glaser, J. Cai, L. Jepeal, D. S. Walton, and R. L. Maas. 1994. “Two Independent and Interactive DNA-Binding Subdomains of the Pax6 Paired Domain Are Regulated by Alternative Splicing.” *Genes & Development* 8 (17): 2022–34.

Furukawa, T., E. M. Morrow, and C. L. Cepko. 1997. “Crx, a Novel Otx-like Homeobox Gene, Shows Photoreceptor-Specific Expression and Regulates Photoreceptor Differentiation.” *Cell* 91 (4): 531–41.

Georgala, Petrina A., Catherine B. Carr, and David J. Price. 2011. “The Role of Pax6 in Forebrain Development.” *Developmental Neurobiology* 71 (8): 690–709.

George, Sophia H. L., Marina Gertsenstein, Kristina Vintersten, Ella Korets-Smith, John Murphy, Mary E. Stevens, Jody J. Haigh, and Andras Nagy. 2007. “Developmental and Adult Phenotyping Directly from Mutant Embryonic Stem Cells.” *Proceedings of the National Academy of Sciences of the United States of America* 104 (11): 4455–60.

Goudreau, Guy, Petros Petrou, Lixing W. Reneker, Jochen Graw, Jana Löster, and Peter Gruss. 2002. “Mutually Regulated Expression of Pax6 and Six3 and Its Implications for the Pax6 Haploinsufficient Lens Phenotype.” *Proceedings of the National Academy of Sciences of the United States of America* 99 (13): 8719–24.

Hart, Alan W., Sebastien Mella, Jacek Mendrychowski, Veronica van Heyningen, and Dirk A. Kleinjan. 2013. “The Developmental Regulator Pax6 Is Essential for Maintenance of Islet Cell Function in the Adult Mouse Pancreas.” *PLoS ONE*. https://doi.org/10.1371/journal.pone.0054173.

Hart, A. W., N. Baeza, A. Apelqvist, and H. Edlund. 2000. “Attenuation of FGF Signalling in Mouse Beta-Cells Leads to Diabetes.” *Nature* 408 (6814): 864–68.

Hill, R. E., J. Favor, B. L. Hogan, C. C. Ton, G. F. Saunders, I. M. Hanson, J. Prosser, T. Jordan, N. D. Hastie,

and V. van Heyningen. 1991. “Mouse Small Eye Results from Mutations in a Paired-like Homeobox-Containing Gene.” *Nature* 354 (6354): 522–25.

Hoang, Thanh V., Evan R. Horowitz, Blake R. Chaffee, Peipei Qi, Rachel E. Flake, Devin G. Bruney, Blake J. Rasor, Savana E. Rosalez, Brad D. Wagner, and Michael L. Robinson. 2017. “Lens Development Requires DNMT1 but Takes Place Normally in the Absence of Both DNMT3A and DNMT3B Activity.” *Epigenetics*. https://doi.org/10.1080/15592294.2016.1253651.

Inoue, Toshihiro, Tetsushi Kagawa, Miyuki Inoue-Mochita, Kyoichi Isono, Naoki Ohtsu, Ikuo Nobuhisa, Mikiko Fukushima, Hidenobu Tanihara, and Tetsuya Taga. 2010. “Involvement of the Hipk Family in Regulation of Eyeball Size, Lens Formation and Retinal Morphogenesis.” *FEBS Letters*. https://doi.org/10.1016/j.febslet.2010.06.020.

Kim, Eun A., Yoon Tae Noh, Myung-Jeom Ryu, Hyun-Taek Kim, Sung-Eun Lee, Cheol-Hee Kim, Cheolju Lee, Young Ho Kim, and Cheol Yong Choi. 2006. “Phosphorylation and Transactivation of Pax6 by Homeodomain-Interacting Protein Kinase 2.” *The Journal of Biological Chemistry* 281 (11): 7489–97.

Klimova, Lucie, and Zbynek Kozmik. 2014. “Stage-Dependent Requirement of Neuroretinal Pax6 for Lens and Retina Development.” *Development* 141 (6): 1292–1302.

Lambert, Wendi S., Silvia Pasini, John W. Collyer, Cathryn R. Formichella, Purnima Ghose, Brian J. Carlson, and David J. Calkins. 2020. “Of Mice and Monkeys: Neuroprotective Efficacy of the p38 Inhibitor BIRB 796 Depends on Model Duration in Experimental Glaucoma.” *Scientific Reports* 10 (1): 8535.

Lefebvre, Tony, Nathalie Planque, Denis Leleu, Manuella Bailly, Marie-Laure Caillet-Boudin, Simon Saule, and Jean-Claude Michalski. 2002. “O-Glycosylation of the Nuclear Forms of Pax-6 Products in Quail Neuroretina Cells.” *Journal of Cellular Biochemistry*. https://doi.org/10.1002/jcb.10119.

Lillie, J. W., and M. R. Green. 1989. “Transcription Activation by the Adenovirus E1a Protein.” *Nature* 338 (6210): 39–44.

Machon, Ondrej, Jana Kreslova, Jana Ruzickova, Tomas Vacik, Lucie Klimova, Naoko Fujimura, Jitka Lachova, and Zbynek Kozmik. 2009. “Lens Morphogenesis Is Dependent on Pax6-Mediated Inhibition of the Canonical Wnt/beta-Catenin Signaling in the Lens Surface Ectoderm.” *Genesis*. https://doi.org/10.1002/dvg.20583.

Mikkola, I., J. A. Bruun, G. Bjorkoy, T. Holm, and T. Johansen. 1999. “Phosphorylation of the Transactivation Domain of Pax6 by Extracellular Signal-Regulated Kinase and p38 Mitogen-Activated Protein Kinase.” *The Journal of Biological Chemistry* 274 (21): 15115–26.

Nishimura, Darryl. 2002. “Faculty Opinions Recommendation of Iris Hypoplasia in Mice That Lack the Alternatively Spliced Pax6(5a) Isoform.” *Faculty Opinions – Post-Publication Peer Review of the Biomedical Literature*. https://doi.org/10.3410/f.1006660.84156.

Nishizawa, K., and H. Okamoto. 1994. “Mutation Analysis of the Role for the Carboxy-Terminus Encoding Region in NGF-Induced Stabilization of GAP-43 mRNA.” *Biochemical and Biophysical Research Communications* 205 (2): 1380–85.

Oron-Karni, Varda, Chen Farhy, Michael Elgart, Till Marquardt, Lena Remizova, Orly Yaron, Qing Xie, Ales Cvekl, and Ruth Ashery-Padan. 2008. “Dual Requirement for Pax6 in Retinal Progenitor Cells.” *Development* 135 (24): 4037–47.

Padula, Stephanie L., Deepti Anand, Thanh V. Hoang, Blake R. Chaffee, Lin Liu, Chun Liang, Salil A. Lachke, and Michael L. Robinson. 2019. “High-Throughput Transcriptome Analysis Reveals That the Loss of Pten Activates a Novel NKX6-1/RASGRP1 Regulatory Module to Rescue Microphthalmia Caused by Fgfr2-Deficient Lenses.” *Human Genetics* 138 (11-12): 1391–1407.

Panneerselvam, Antojenifer, Arun Kannan, Lezy Flora Mariajoseph-Antony, and Chidambaram Prahalathan. 2019. “PAX Proteins and Their Role in Pancreas.” *Diabetes Research and Clinical Practice* 155 (September): 107792.

Quinn, Jane C., Michael Molinek, Ben S. Martynoga, Paulette A. Zaki, Andrea Faedo, Alessandro Bulfone,

Robert F. Hevner, John D. West, and David J. Price. 2007. “Pax6 Controls Cerebral Cortical Cell Number by Regulating Exit from the Cell Cycle and Specifies Cortical Cell Identity by a Cell Autonomous Mechanism.” *Developmental Biology* 302 (1): 50–65.

Ran, F. Ann, Patrick D. Hsu, Chie-Yu Lin, Jonathan S. Gootenberg, Silvana Konermann, Alexandro E. Trevino, David A. Scott, et al. 2013. “Double Nicking by RNA-Guided CRISPR Cas9 for Enhanced Genome Editing Specificity.” *Cell* 154 (6): 1380–89.

Ran, F. Ann, Patrick D. Hsu, Jason Wright, Vineeta Agarwala, David A. Scott, and Feng Zhang. 2013. “Genome Engineering Using the CRISPR-Cas9 System.” *Nature Protocols* 8 (11): 2281–2308.

Reddan, J. R., J. F. Kuck, D. C. Dziedzic, K. D. Kuck, P. R. Reddan, and P. Wasielewski. 1989. “Establishment of Lens Epithelial Cell Lines from Emory and Cataract Resistant Mice and Their Response to Hydrogen Peroxide.” *Lens and Eye Toxicity Research* 6 (4): 687–701.

Remez, Liv Aleen, Akishi Onishi, Yotam Menuchin-Lasowski, Assaf Biran, Seth Blackshaw, Karl J. Wahlin, Donlad J. Zack, and Ruth Ashery-Padan. 2017. “Pax6 Is Essential for the Generation of Late-Born Retinal Neurons and for Inhibition of Photoreceptor-Fate during Late Stages of Retinogenesis.” *Developmental Biology* 432 (1): 140–50.

Roberts, R. C. 1967. “Small Eyes—a New Dominant Eye Mutant in the Mouse.” *Genetics Research* 9 (1): 121–22.

Ross, J. 1995. “mRNA Stability in Mammalian Cells.” *Microbiological Reviews* 59 (3): 423–50.

Sander, M., A. Neubüser, J. Kalamaras, H. C. Ee, G. R. Martin, and M. S. German. 1997. “Genetic Analysis Reveals That PAX6 Is Required for Normal Transcription of Pancreatic Hormone Genes and Islet Development.” *Genes & Development* 11 (13): 1662–73.

Sanjaya Singh, Rajnikant Mishra, Nelson A. Arango, Jian Min Deng, Richard R. Behringer, and Grady F. Saunders. 2002. “Iris Hypoplasia in Mice That Lack the Alternatively Spliced Pax6(5a) Isoform.” PNAS. April 30, 2002. https://www.pnas.org/content/pnas/99/10/6812.

Sansom, Stephen N., Dean S. Griffiths, Andrea Faedo, Dirk-Jan Kleinjan, Youlin Ruan, James Smith, Veronica van Heyningen, John L. Rubenstein, and Frederick J. Livesey. 2009. “The Level of the Transcription Factor Pax6 Is Essential for Controlling the Balance between Neural Stem Cell Self-Renewal and Neurogenesis.” *PLoS Genetics*. https://doi.org/10.1371/journal.pgen.1000511.

Schwarz, M., F. Cecconi, G. Bernier, N. Andrejewski, B. Kammandel, M. Wagner, and P. Gruss. 2000. “Spatial Specification of Mammalian Eye Territories by Reciprocal Transcriptional Repression of Pax2 and Pax6.” *Development* 127 (20): 4325–34.

Sekiya, Takashi, and Kenneth S. Zaret. 2007. “Repression by Groucho/TLE/Grg Proteins: Genomic Site Recruitment Generates Compacted Chromatin In Vitro and Impairs Activator Binding In Vivo.” *Molecular Cell*. https://doi.org/10.1016/j.molcel.2007.10.002.

Shaham, Ohad, April N. Smith, Michael L. Robinson, Makoto M. Taketo, Richard A. Lang, and Ruth Ashery-Padan. 2009. “Pax6 Is Essential for Lens Fiber Cell Differentiation.” *Development* 136 (15): 2567–78.

Sun, Jian, Shira Rockowitz, Qing Xie, Ruth Ashery-Padan, Deyou Zheng, and Ales Cvekl. 2015. “Identification of in Vivo DNA-Binding Mechanisms of Pax6 and Reconstruction of Pax6-Dependent Gene Regulatory Networks during Forebrain and Lens Development.” *Nucleic Acids Research* 43 (14): 6827–46.

Sun, Jian, Yilin Zhao, Rebecca McGreal, Yamit Cohen-Tayar, Shira Rockowitz, Carola Wilczek, Ruth Ashery-Padan, David Shechter, Deyou Zheng, and Ales Cvekl. 2016. “Pax6 Associates with H3K4-Specific Histone Methyltransferases Mll1, Mll2, and Set1a and Regulates H3K4 Methylation at Promoters and Enhancers.” *Epigenetics & Chromatin* 9 (1): 37.

Swisa, Avital, Dana Avrahami, Noa Eden, Jia Zhang, Eseye Feleke, Tehila Dahan, Yamit Cohen-Tayar, et al. 2017. “PAX6 Maintains β Cell Identity by Repressing Genes of Alternative Islet Cell Types.” *The Journal of Clinical Investigation* 127 (1): 230–43.

Terrell, Anne M., Deepti Anand, Sylvie F. Smith, Christine A. Dang, Stephanie M. Waters, Mallika Pathania, David C. Beebe, and Salil A. Lachke. 2015. “Molecular Characterization of Mouse Lens Epithelial Cell Lines and Their Suitability to Study RNA Granules and Cataract Associated Genes.” *Experimental Eye Research*. https://doi.org/10.1016/j.exer.2014.12.011.

Titford, Michael. 2009. “Progress in the Development of Microscopical Techniques for Diagnostic Pathology.” *Journal of Histotechnology* 32 (1): 9–19.

Toresson, H., S. S. Potter, and K. Campbell. 2000. “Genetic Control of Dorsal-Ventral Identity in the Telencephalon: Opposing Roles for Pax6 and Gsh2.” *Development* 127 (20): 4361–71.

Treisman, J., E. Harris, and C. Desplan. 1991. “The Paired Box Encodes a Second DNA-Binding Domain in the Paired Homeo Domain Protein.” *Genes & Development* 5 (4): 594–604.

Tuoc, Tran Cong, and Anastassia Stoykova. 2008. “Trim11 Modulates the Function of Neurogenic Transcription Factor Pax6 through Ubiquitin–proteosome System.” *Genes & Development* 22 (14): 1972–86.

Walther, C., and P. Gruss. 1991. “Pax-6, a Murine Paired Box Gene, Is Expressed in the Developing CNS.” *Development* 113 (4): 1435–49.

Washington, Nicole L., Melissa A. Haendel, Christopher J. Mungall, Michael Ashburner, Monte Westerfield, and Suzanna E. Lewis. 2009. “Linking Human Diseases to Animal Models Using Ontology-Based Phenotype Annotation.” *PLoS Biology* 7 (11): e1000247.

Wolf, Louise V., Ying Yang, Jinhua Wang, Qing Xie, Barbara Braunger, Ernst R. Tamm, Jiri Zavadil, and Ales Cvekl. 2009. “Identification of pax6-Dependent Gene Regulatory Networks in the Mouse Lens.” *PloS One* 4 (1): e4159.

Wong, Rebecca Lee Yean, and King Lau Chow. 2002. “Depletion of Mab21l1 and Mab21l2 Messages in Mouse Embryo Arrests Axial Turning, and Impairs Notochord and Neural Tube Differentiation.” *Teratology* 65 (2): 70–77.

Xie, Qing, and Ales Cvekl. 2011. “The Orchestration of Mammalian Tissue Morphogenesis through a Series of Coherent Feed-Forward Loops.” *The Journal of Biological Chemistry* 286 (50): 43259–71.

Xie, Qing, Ying Yang, Jie Huang, Jovica Ninkovic, Tessa Walcher, Louise Wolf, Ariel Vitenzon, et al. 2013. “Pax6 Interactions with Chromatin and Identification of Its Novel Direct Target Genes in Lens and Forebrain.” *PloS One* 8 (1): e54507.

Xu, H. E., M. A. Rould, W. Xu, J. A. Epstein, R. L. Maas, and C. O. Pabo. 1999. “Crystal Structure of the Human Pax6 Paired Domain-DNA Complex Reveals Specific Roles for the Linker Region and Carboxy-Terminal Subdomain in DNA Binding.” *Genes & Development*. https://doi.org/10.1101/gad.13.10.1263.

Xu, W., M. A. Rould, S. Jun, C. Desplan, and C. O. Pabo. 1995. “Crystal Structure of a Paired Domain-DNA Complex at 2.5 Angstroms Resolution Reveals Structural Basis for Pax Developmental Mutations.” Worldwide Protein Data Bank. https://doi.org/10.2210/pdb1pdn/pdb.

Yang, Ying, Bharesh K. Chauhan, Kveta Cveklova, and Ales Cvekl. 2004. “Transcriptional Regulation of Mouse αB- and γF-Crystallin Genes in Lens: Opposite Promoter-Specific Interactions Between Pax6 and Large Maf Transcription Factors.” *Journal of Molecular Biology*. https://doi.org/10.1016/j.jmb.2004.07.102.

Yan, Qin, Lili Gong, Mi Deng, Lan Zhang, Shuming Sun, Jiao Liu, Haili Ma, et al. 2010. “Sumoylation Activates the Transcriptional Activity of Pax-6, an Important Transcription Factor for Eye and Brain Development.” *Proceedings of the National Academy of Sciences of the United States of America* 107 (49): 21034–39.

Yan, Qin, Wen-Bin Liu, Jichao Qin, Jinping Liu, He-Ge Chen, Xiaoqin Huang, Lili Chen, et al. 2007. “Protein Phosphatase-1 Modulates the Function of Pax-6, a Transcription Factor Controlling Brain and Eye Development.” *The Journal of Biological Chemistry* 282 (19): 13954–65.

Yu, Fei, Weijie Zhang, Chenxi Yan, Dan Yan, Meng Zhou, Junzhao Chen, Xiangteng Zhao, et al. 2020.

"PAX6, Modified by SUMOylation, Plays a Protective Role in Corneal Endothelial Injury." *Cell Death & Disease* 11 (8): 683.
Yun, K., S. Potter, and J. L. Rubenstein. 2001. "Gsh2 and Pax6 Play Complementary Roles in Dorsoventral Patterning of the Mammalian Telencephalon." *Development* 128 (2): 193–205.

Figures and Tables

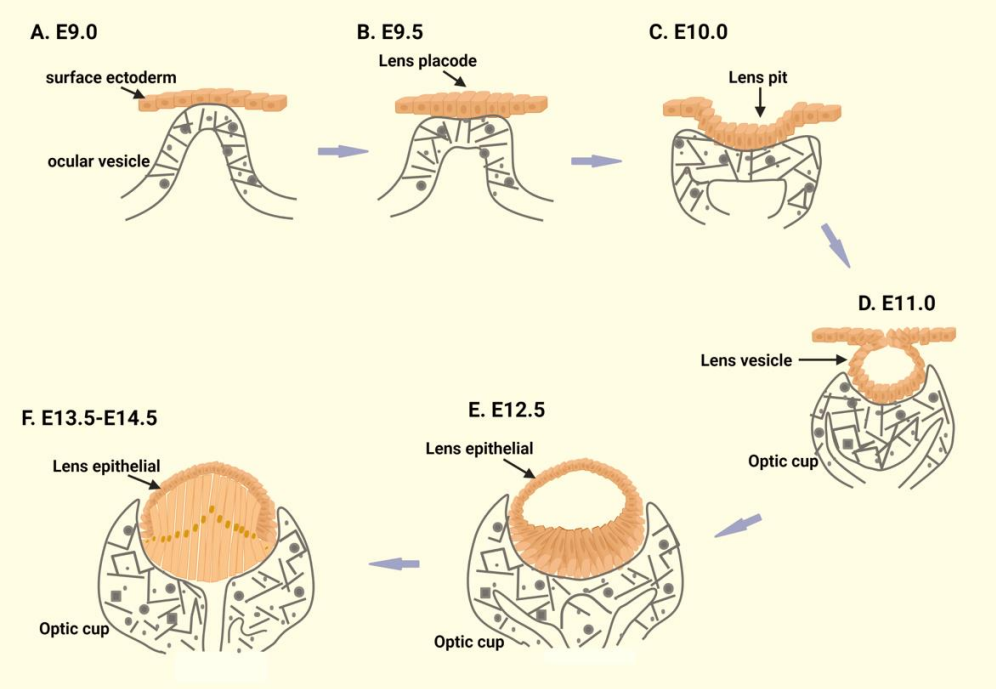

Figure 1. The brief depiction of mouse lens development (Cvekl and Ashery-Padan 2014). Photo was created using the software BioRender.

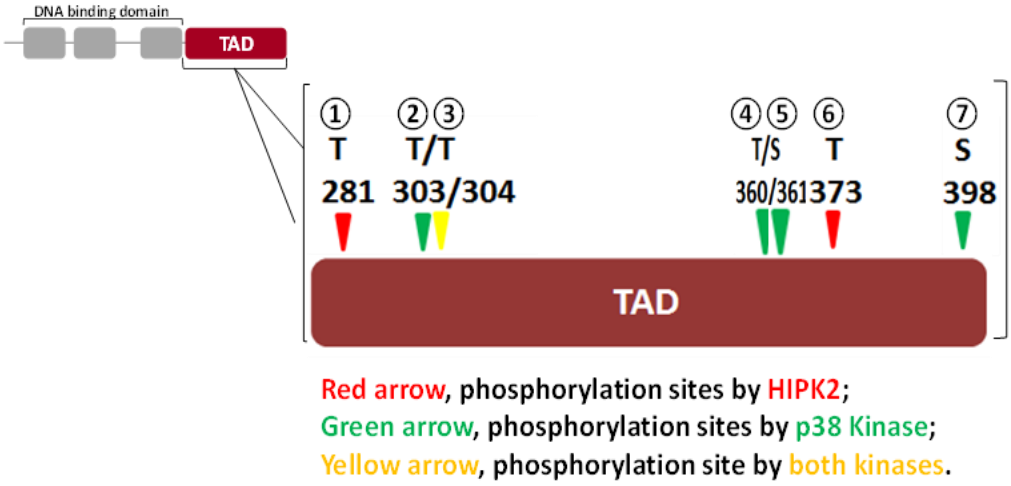

Figure 2. Map of 7 phosphorylation sites on TAD of murine PAX6 catalyzed by HIPK2 and p38 kinases. All the sites were labeled numerically by order.

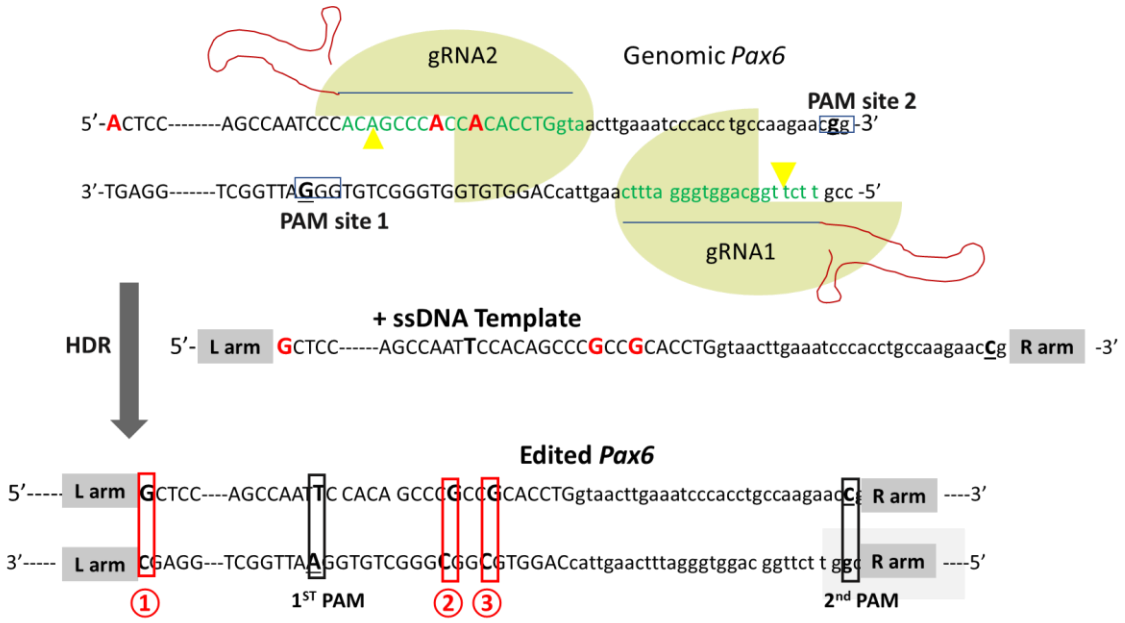

Figure 3. Double nicking by RNA-guided CRISPR Cas9 nickase to mutate the first three phosphorylation-sites of *Pax6* TAD.

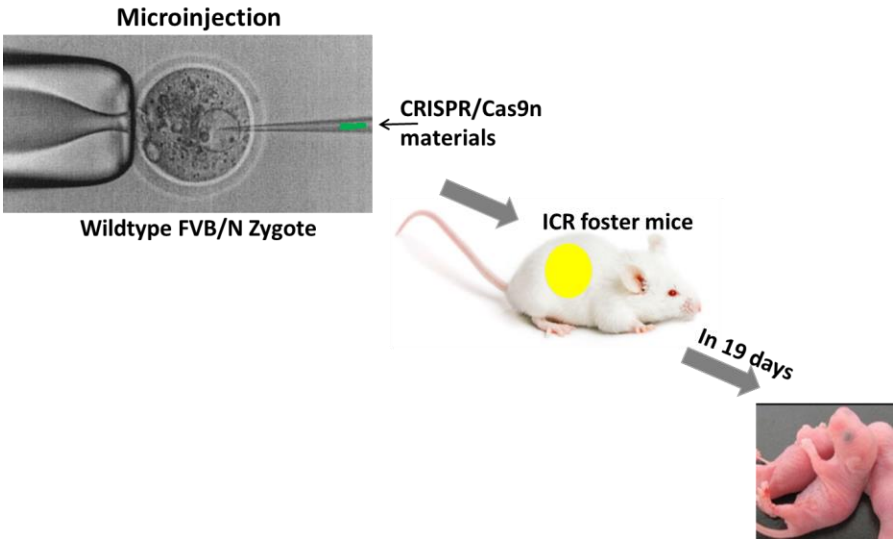

Figure 4. Flow chart of generating transgenic mouse model.

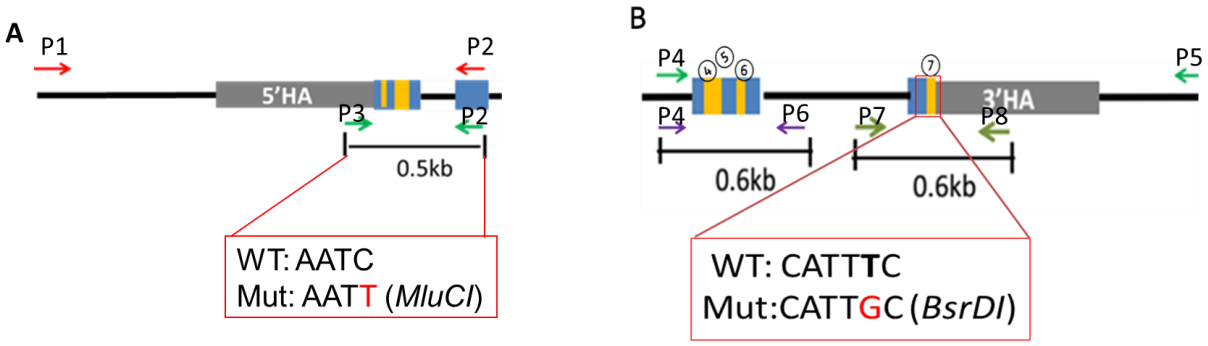

Figure 5. Schematic representation of genotyping PCR plan on the PAX6 TAD mutant mice.
A, two rounds of PCR reactions were performed to test the mutations of Site 1-3 located at the 5'end of the targeted DNA. Firstly, to ensure the tested DNA located on the expected position, one of the primers was designed to bind to the upstream DNA of 5'HA (Homology Arm) and the reverse primer targets the downstream DNA of Site 3. Next, using PCR product as the template, the DNA copies with a size of about 0.5kb were obtained in the second PCR for sequencing. Compared with the wildtype sequence, a novel restriction site of *MluCI* was introduced within the DNA region of 0.5kb in size if the first PAM site was mutated properly. B, two rounds of PCR reactions were done to examine the mutations of Site 4-6 and Site 7 located at the 3'end. The first PCR product was gained with the reverse primer targeting the downstream DNA of 3'HA. In the next round of PCR, the DNA copies containing the Site 4-6 and the Site 7 mutations, was produced respectively, based on the first PCR product above. Compared with the wildtype sequence, a novel restriction site of *BsrDI*, was introduced within the DNA region of 0.6kb in size if Site 7 was mutated properly. WT, wildtype sequence; Mut, mutated phosphorylation-site sequence.

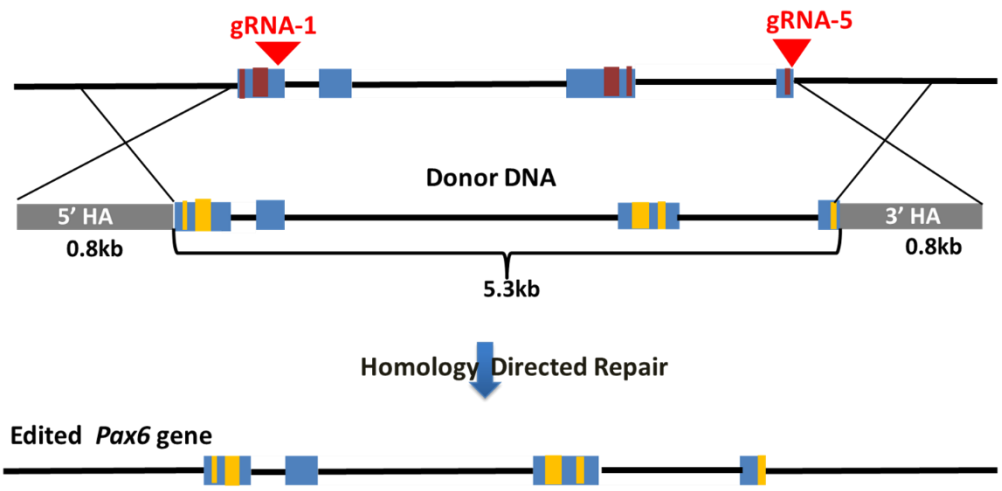

Figure 6. Diagram of creating zygotes with *Pax6* seven phosphorylation site mutations through CRISPR/Cas9 using SgRNA 1 and 5. 5' HA, 5' Homology arm; 3'HA, 3' Homology arm.

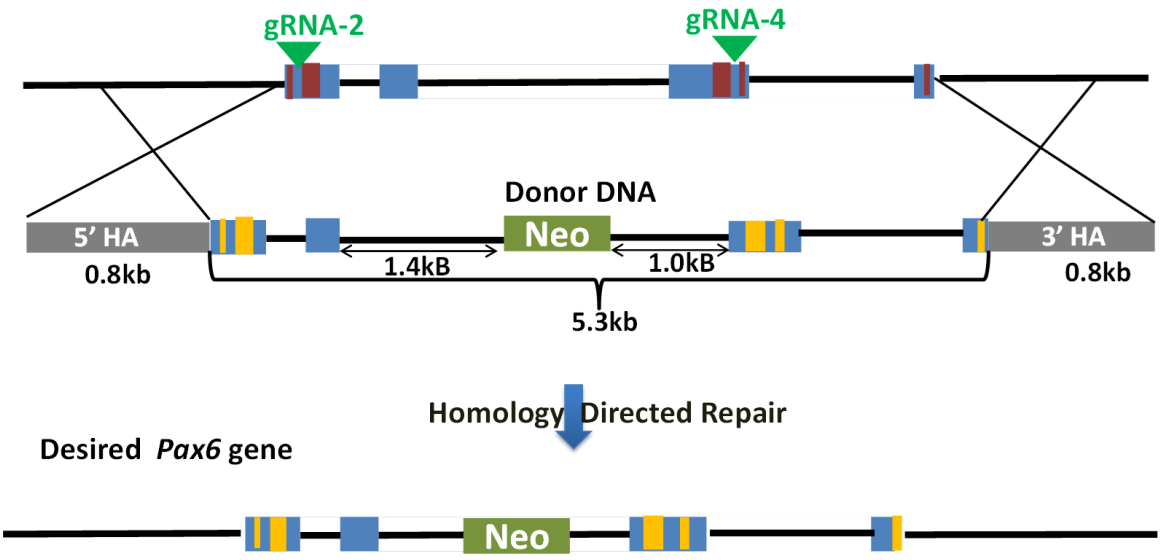

Figure 7. Schematic depicting the generation mouse stem cells with *Pax6* seven phosphorylation site mutations through CRISPR/Cas9 system using SgRNA 2 and 4. 5' HA, 5' Homology arm; 3'HA, 3' Homology arm; Neo, neomycin-resistant gene.

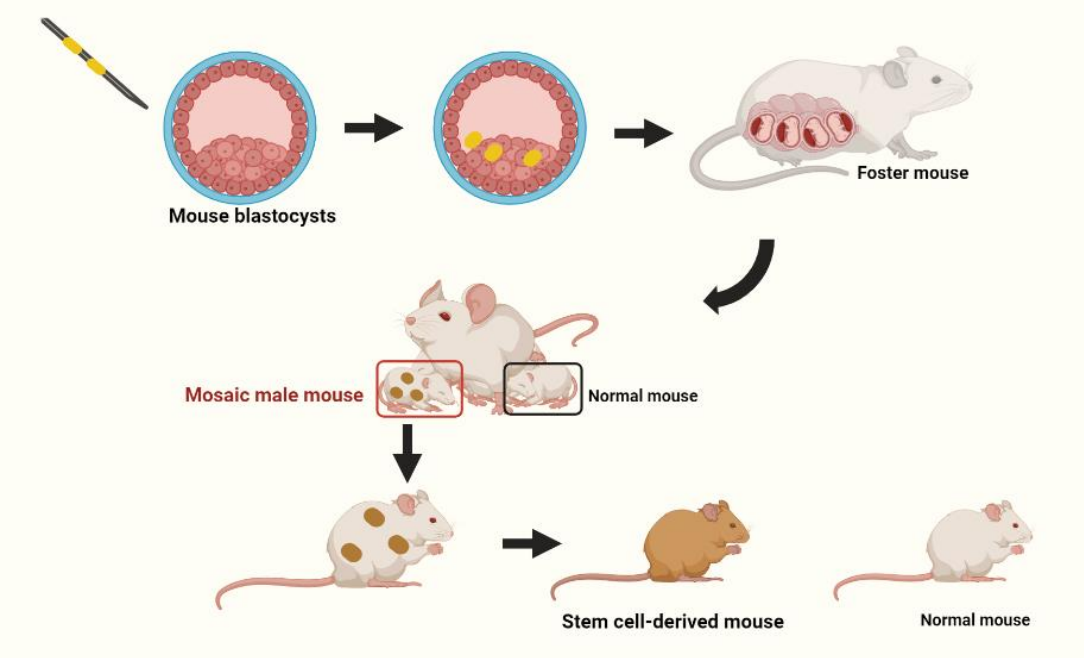

Figure 8. Flow chart of generating ES-derived transgenic mouse lines. Mutate mouse stem cells were injected into early blastocysts and then transimplanted into ICR foster mice for chimeric offspring. Finally, the mosaic mice were bred with wildtype FVB/N mice to gain the pure stem cell-derived mutants. Photo was created using the software BioRender.

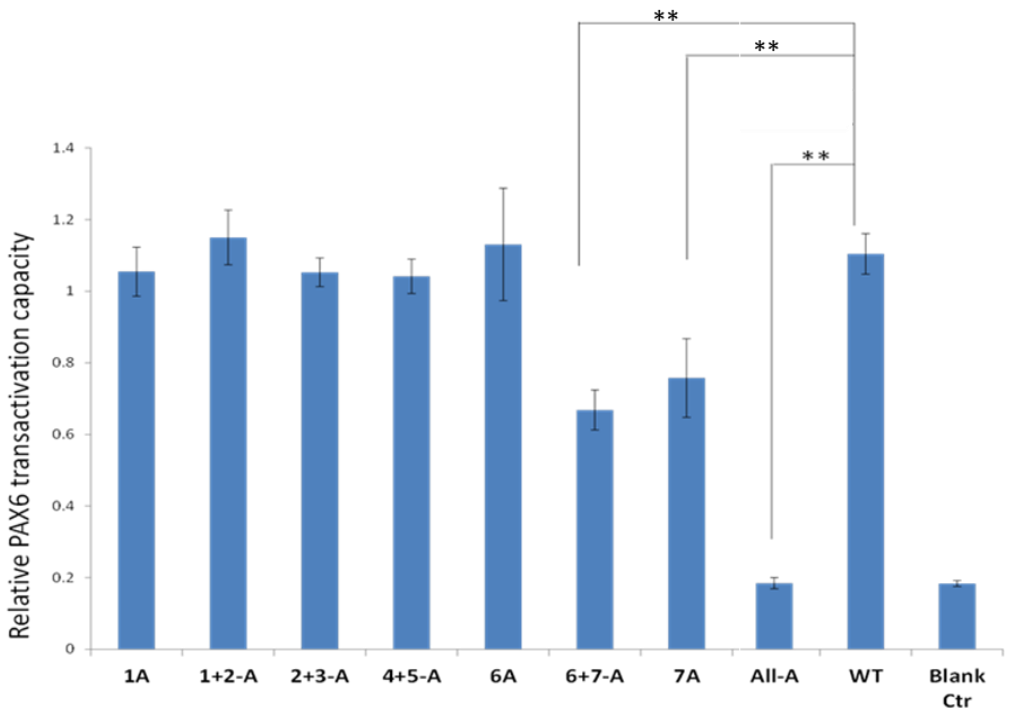

Figure 9. Examination of the effects of phosphorylation sites on transactivation potential of PAX6 through Luciferase *in vitro* assays. PAX6 transactivation activity differences were determined by measuring the ratios of firefly luciferase over renilla luciferase from MK4 (mouse Kidney 4) cells that were co-transfected with plasmid DNA containing a PAX6-inducible promoter (called Cignal Reporter) and the plasmid with mutated *Pax6* cDNA on phosphorylation site(s) into alanine(s); Blank Ctr, just Cignal Reporter DNA was transfected into cells; WT, wildtype *Pax6* cDNA, along with Cignal Reporter; 1,2-A, *Pax6* plasmid with both Site 1 and 2 mutated into alanine and Cignal Reporter; 2,3-A, Site 2 and 3 inactivated; 4,5-A, Site 2 and 3 altered ; 6A, Site 6 mutated; 6,7-A, Site 6 and 7 changed; All-A, all 7 sites mutated; WT, *Pax6* plasmid with all 7 sites unaltered and Cignal Reporter.

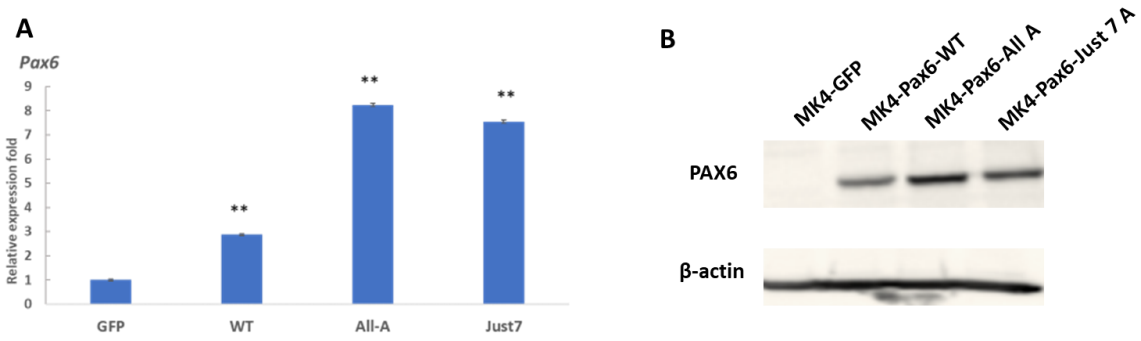

Figure 10. The overexpression wildtype and mutated *Pax6* in MK4 cells were examined through RT-qPCR and Western blot assays.

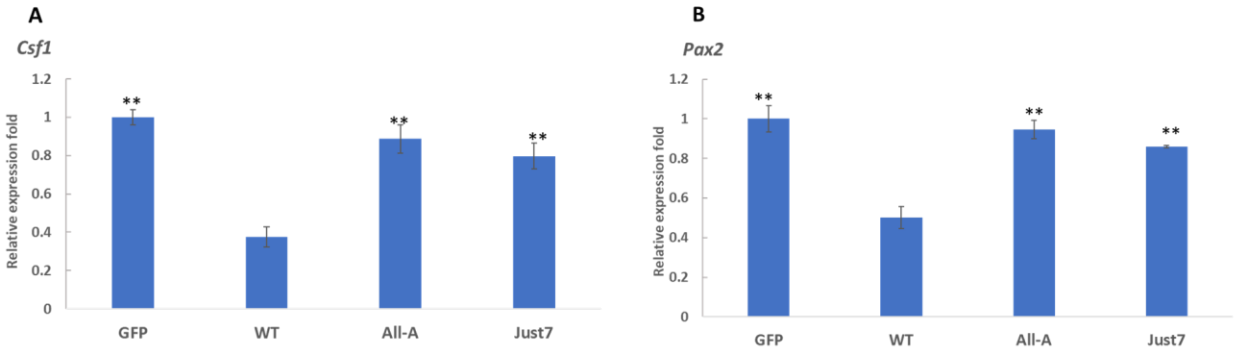

Figure 11. The RT-qPCR assays demonstrated that the repression of *Csf1* and *Pax2* expression was abolished by Pax6 with Site-7 mutation, especially when all seven sites were destroyed in MK4 cells. To determine if the repressive target genes, *Csf1* and *Pax2*, were regulated by PAX6 TAD phosphorylation, wildtype or phosphorylation-site mutated plasmid DNA was transfected into MK4 cells, respectively. After 36 hours, cells would be harvested for RT-PCR to detect the mRNA levels of target genes, in contrast to that of GFP control group. GFP, GFP construct; WT, wildtype Pax6 cDNA; Just 7, site 7 changed into A; All-A, all 7 sites mutated.

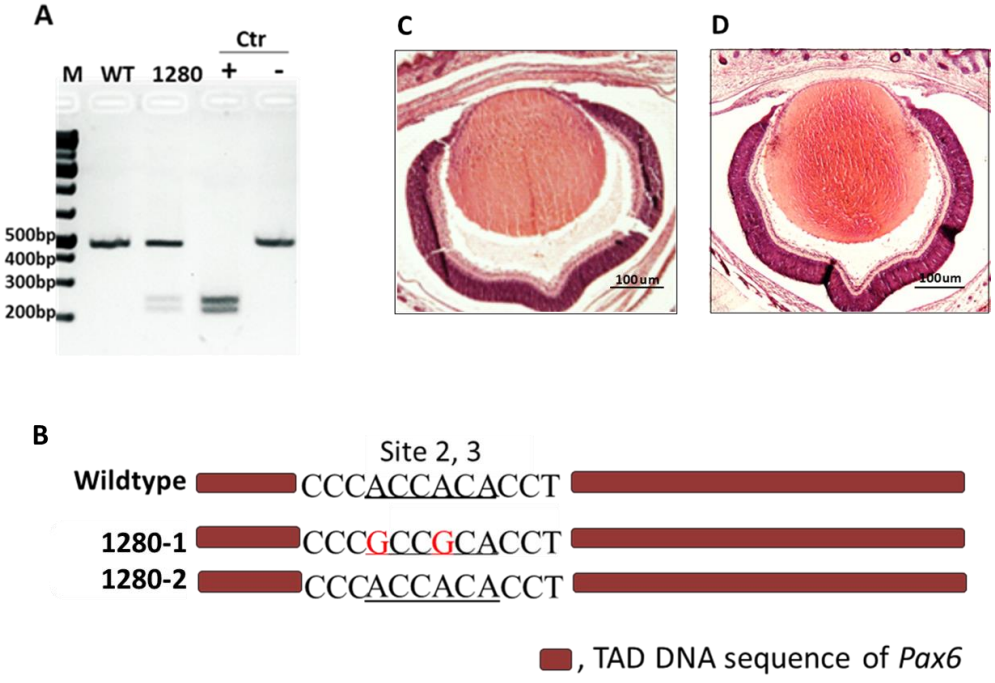

Figure 12. Analysis of founder mouse 1280 with mutations on 2nd and 3rd sites. A, mutated DNA could be cleaved by the restriction enzyme *MluCI*; B, the sequencing analysis of 1280 with one allele mutated (ACCA into GCCG) and the other not; C and D, histology staining analysis on lens of newborn wildtype (FVB/N) and the homozygous mutant, respectively.

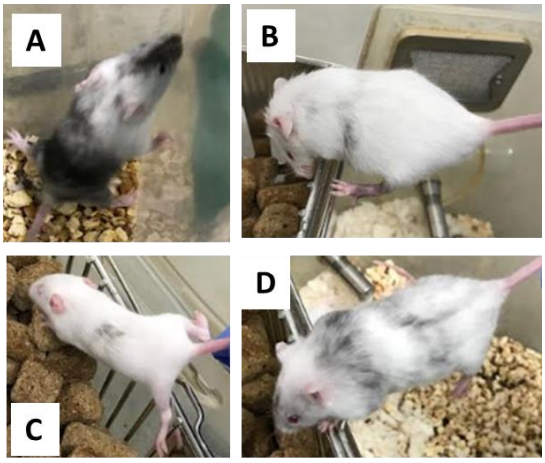

Figure 13. Four Clone-67-derived chimeric mice. Mouse B was male, and the rest three mice were females.

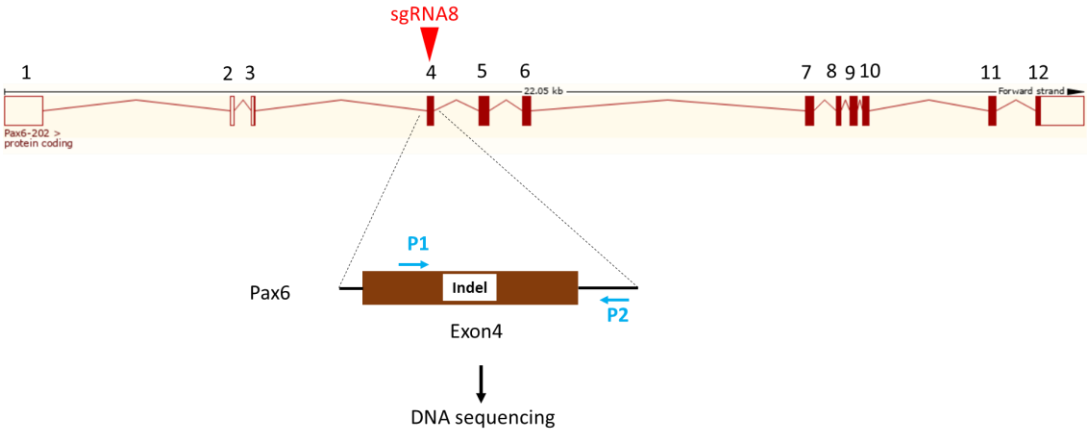

Figure 14. Schematic representation of creating Pax6-null cell line via CRISPR/CAS9 technique. For the sequence information of P1 and P2 was listed in Table 7.

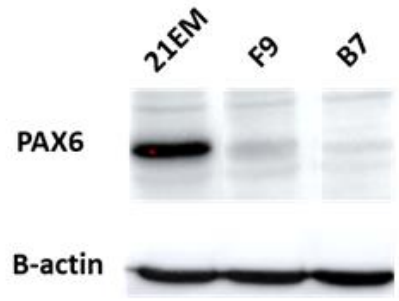

Figure 15. Deletion of *Pax6* in Clone F9 and B7 was verified in Western blot.

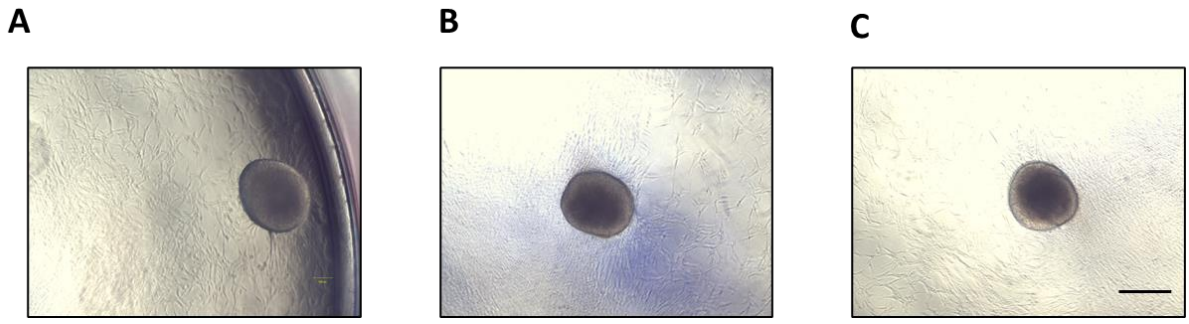

Figure 16. No obvious difference was seen in the comparison of lentoid body formation between wildtype and mutated 21EM15 cells. A, wildtype 21EM15 cells; B, F9 mutant cells; C, B7 mutant cells. Scale bar=100um.

Table 1 Summary of primers to create *Pax6* phosphorylation-site alanine substitution mutations in pMXs-*Pax6*

Primer Name	Sequence
Site 1 mutated Forward	aagacaggccagcaacgctcctagtcacattcc
Site 1 mutated Reverse	ggaatgtgactaggagcgttgctggcctgtctt
Site 2,3 mutated Forward	caatcccacagcccgccgcacctgtctcctcc
Site 2,3 mutated Reverse	ggaggagacaggtgcggcgggctgtgggattg
Site 4,5 mutated Forward	cgtgcatgctgcccgccgccccgtcagtgaatg
Site 4,5 mutated Reverse	cattcactgacggggcggcgggcagcatgcacg
Site 7 mutated Forward	acttcaacaggactcattgcacctggagtgtcagt
Site 7 mutated Reverse	actgacactccaggtgcaatgagtcctgttgaagt

Table 2 Sequence of wildtype and mutated pMXs-Pax6

Name	cDNA Seq
Wildtype *Pax6* in pMXs-*Pax6* *	ATGCAGAACAGTCACAGCGGAGTGAATCAGCTTGGTGGTGTCTTTGTCAACGGGCGGCCACTGCCGG ACTCCACCCGGCAGAAGATCGTAGAGCTAGCTCACAGCGGGGCCCGGCCGTGCGACATTTCCCGAAT TCTGCAGGTATCCAACGGTTGTGTGAGTAAAATTCTGGGCAGGTATTACGAGACTGGCTCCATCAGA CCCAGGGCAATCGGAGGGAGTAAGCCAAGAGTGGCGACTCCAGAAGTTGTAAGCAAAATAGCCCAG TATAAACGGGAGTGCCCTTCCATCTTTGCTTGGGAAATCCGAGACAGATTATTATCCGAGGGGGTCT GTACCAACGATAACATACCCAGTGTGTCATCAATAAACAGAGTTCTTCGCAACCTGGCTAGCGAAAA GCAACAGATGGGCGCAGACGGCATGTATGATAAACTAAGGATGTTGAACGGGCAGACCGGAAGCTG GGGCACACGCCCTGGTTGGTATCCCGGGACTTCAGTACCAGGGCAACCCACGCAAGATGGCTGCCA GCAACAGGAAGGAGGGGGAGAGAACACCAACTCCATCAGTTCTAACGGAGAAGACTCGGATGAAG CTCAGATGCGACTTCAGCTGAAGCGGAAGCTGCAAAGAAATAGAACATCTTTTACCCAAGAGCAGA TTGAGGCTCTGGAGAAAGAGTTTGAGAGGACCCATTATCCAGATGTGTTTGCCCGGGAAAGACTAGC AGCCAAAATAGATCTACCTGAAGCAAGAATACAGGTATGGTTTTCTAATCGAAGGGCCAAATGGAG AAGAGAAGAGAAACTGAGGAACCAGAGAAGACAGGCCAGCAACACTCCTAGTCACATTCCTATCAG CAGCAGCTTCAGTACCAGTGTCTACCAGCCAATCCCACAGCCCACCACACCTGTCTCCTCCTTCACAT CAGGTTCCATGTTGGGCCGAACAGACACCGCCCTCACCAACACGTACAGTGCTTTGCCACCCATGCC CAGCTTCACCATGGCAAACAACCTGCCTATGCAACCCCCAGTCCCCAGTCAGACCTCCTCATACTCG TGCATGCTGCCCACCAGCCCGTCAGTGAATGGGCGGAGTTATGATACCTACACCCCTCCGCACATGC AAACACACATGAACAGTCAGCCCATGGGCACCTCGGGGACCACTTCAACAGGACTCATTTCACCTGG AGTGTCAGTTCCCGTCCAAGTTCCCGGGAGTGAACCTGACATGTCTCAGTACTGGCCTCGATTACAG TAA
Pax6 with seven-site-substitution mutation in pMXs-*Pax6* *	ATGCAGAACAGTCACAGCGGAGTGAATCAGCTTGGTGGTGTCTTTGTCAACGGGCGGCCACTGCCGG ACTCCACCCGGCAGAAGATCGTAGAGCTAGCTCACAGCGGGGCCCGGCCGTGCGACATTTCCCGAAT TCTGCAGGTATCCAACGGTTGTGTGAGTAAAATTCTGGGCAGGTATTACGAGACTGGCTCCATCAGA CCCAGGGCAATCGGAGGGAGTAAGCCAAGAGTGGCGACTCCAGAAGTTGTAAGCAAAATAGCCCAG TATAAACGGGAGTGCCCTTCCATCTTTGCTTGGGAAATCCGAGACAGATTATTATCCGAGGGGGTCT GTACCAACGATAACATACCCAGTGTGTCATCAATAAACAGAGTTCTTCGCAACCTGGCTAGCGAAAA GCAACAGATGGGCGCAGACGGCATGTATGATAAACTAAGGATGTTGAACGGGCAGACCGGAAGCTG GGGCACACGCCCTGGTTGGTATCCCGGGACTTCAGTACCAGGGCAACCCACGCAAGATGGCTGCCA GCAACAGGAAGGAGGGGGAGAGAACACCAACTCCATCAGTTCTAACGGAGAAGACTCGGATGAAG CTCAGATGCGACTTCAGCTGAAGCGGAAGCTGCAAAGAAATAGAACATCTTTTACCCAAGAGCAGA TTGAGGCTCTGGAGAAAGAGTTTGAGAGGACCCATTATCCAGATGTGTTTGCCCGGGAAAGACTAGC AGCCAAAATAGATCTACCTGAAGCAAGAATACAGGTATGGTTTTCTAATCGAAGGGCCAAATGGAG AAGAGAAGAGAAACTGAGGAACCAGAGAAGACAGGCCAGCAACGCTCCTAGTCACATTCCTATCAG CAGCAGCTTCAGTACCAGTGTCTACCAGCCAATCCCACAGCCCGCCGCACCTGTCTCCTCCTTCACAT CAGGTTCCATGTTGGGCCGAACAGACACCGCCCTCACCAACACGTACAGTGCTTTGCCACCCATGCC CAGCTTCACCATGGCAAACAACCTGCCTATGCAACCCCCAGTCCCCAGTCAGACCTCCTCATACTCG TGCATGCTGCCCGCCGCCCCGTCAGTGAATGGGCGGAGTTATGATACCTACGCCCCTCCGCACATGC AAACACACATGAACAGTCAGCCCATGGGCACCTCGGGGACCACTTCAACAGGACTCATTGCACCTG GAGTGTCAGTTCCCGTCCAAGTTCCCGGGAGTGAACCTGACATGTCTCAGTACTGGCCTCGATTACA GTAA

*, red and underlined nucleotides are the interesting nucleotides in seven phosphorylation-site substitution mutations.

Table 3 Primers for qPCR

Name	Sequence
Pax2-F	AAGCCCGGAGTGATTGGTG
Pax2-R	CAGGCGAACATAGTCGGGTT
Csf1-F	ATGAGCAGGAGTATTGCCAAGG
Csf1-R	TCCATTCCCAATCATGTGGCTA
Plekha1-F	GACAGAATCGCATCTGTGGA
Plekha1-R	TGAAGGCAGGTTCTGTGGAT
Pax6-F	ACCCGGCAGAAGATCGTAG
Pax6-R	ACCGTTGGATACCTGCAGAA
Gapdh-F	CTTCCGTGTTCCTACCC
Gapdh-R	TGCTGTAGCCGTATTCAT

Table 4 Sequence information of the material in generating *Pax6* Site1-3 mutation transgenic mice

Name	Sequence
SgRNA-1	GAAATCCCACCTGCCAAGAA
SgRNA-2	TACCAGGTGTGGTGGGCTGT
ssDNA repair template*	AATGGAGAAGAGAAGAGAAACTGAGGAACCAGAGAAGACAGGCCAGCAAC GCTCCTAGTCACATTCCTATCAGCAGCAGCTTCAGTACCAGTGTCTACCAGCC AATTCCACAGCCCGCCGCACCTGgtaacttgaaatcccacctgccaagaaccgttcttaacc ttgcctgcccttgactttctcttgccttgtaatgaatgac
Genotyping Forward Primer	ggtttgcaaagactcccttg
Genotyping Reverse Primer	GGTGGCAAAGCACTGTACG

*, red and underlined nucleotides are the interesting nucleotides in seven phosphorylation-site substitution mutations; black and underlined nucleotides are the interesting nucleotides in PAM-site mutations.

Table 5 Sequence information of the material in generating *Pax6* all-site mutation transgenic mice via zygote

Name	Sequence
SgRNA-1	GAAATCCCACCTGCCAAGAA
SgRNA-5	TTCACTCCCGGGAACTTGGA
Repair template*	cagagaaaccttaaatcaaaggaaatgccacagcaaaagcacaaagggctaaatttagctagggctctttgcataaaggatgaaaagccccccccccccactttcagtgtgtgtgt gttttttttttttttgtgtgtgtgtgtgcgcgcatatgcattttctctcttctttttcacacaccagcaaactgaaatattacaattctgacagacaaaggaaatgatgacctatctgactgtctt aggccacagataaggacaaacactaaatgtcattccaaagaaaacttgctcctggtgggaaagttcttgctagtacagtcagcacactgtcaagctgtctgattggctggatgagatg ggagttgggtgttaaaagctaggttgatccagtgtctgaactatcttgtgttctggtataatatataaaatcaacttactctttcag AGTTTGAGAGGACCCATTATCCAGATGTGTTTGCCCGGGAAAGACTAGCAGCCAAAATAGATCTACCTGAAG CAAGAATACAGgtacctagggaccatgtggtttttatgcactgggatgcttatattttgccttggctgtataccagtcactgatataatcatggtcaggtttgcaaagactccct tgttctagggtaagggtggggatggagggcttttgtttgtggccgagtggtagcaagcatagggctaacctgttctgtgcatttccagGTATGGTTTTCTAATCGA AGGGCCAAATGGAGAAGAGAAGAGAAACTGAGGAACCAGAGAAGACAGGCCAGCAACGCTCCTAGTCACA TTCCTATCAGCAGCAGCTTCAGTACCAGTGTCTACCAGCCAATTCCACACAGCCCGCCGCACCTG gtaacttgaaatcccacctgccaagaaccgttcttaaccttgcctgcccttgactttctcttgccttgtaatgaatgaccttgccctctctctgtctctttctcttcctctgcag TCTCCTCCTTCACATCAGGTTCCATGTTGGGCCGAACAGACACCGCCCTCACCAACACGTACAGTGCTTTGCC ACCCATGCCCAGCTTCACCATGGCAAACAACCTGCCTATGCAAgtaagagaggacggtcacctgctgcacagggcaagggatgggttc aggcttgcagacccattcattgcatttactcccttgggagtccttcttgtgacagtgattagcttgaccagtcaactctgagacagtcaatccaacctcttttagctgattgattgactgat tgattgattcatgcccttggaaaacaaacactctatctgttcagtcaagttaatgtgcctttcatcattatgttagctggagaaggccgggcgggcgggagtgaggtcgctttcggctac cagggatgtttgtatcaaagtagaaataattcgggcataatgaaaggtactaaagatgttggcatgtaaaaagtttaggtttacgttagtgggtttgtattaataaatgcagaagcagca caaatattttgaggattacttttggttcctctaagaagctagtgaggaagaggaaaaagggaggggcagctgaaaagcaagattcctctttagagagtgaaatgcatttagtaaaata gggaaactagctccttctacatttaaaagtaaaaatggagtagaaggtatttgctagaaatctaatgtgtgtcagctgtagccgatgtgacaggtcagtggtaacccttgctgcctagg gagctggagggcattcttcctataatacctggcccgtgttcttaggggttggttctggaccaagctggcatggcctagtgtaagttctgcatgactcctggtatgtgctagatcactgtt gcttagaggattctgatgtcttaggaacatcagcaagtcctaaggctcctgctgtacgaccatcagatatgcctgctggtatacgactggaagcatgagccctgctggaagcagttcg ggggaggggttctacagattacttagcctgtactgaacatcttttgccaggcttggaattcaaataacagcaaaataaagtctctcagtcttcaggcctagaactggataagcggtgc cggaggacatattcccctgcttcttttctatggcatctgtcttttattggacatagtgcaactgatgtaaatgaaggggccagcagcccattaagtgggtatggctacaactattttggaat ttcccagaagtcactttgcctagaggaagtgattgcaggaattagaagcaaatgcaagctgaagttctggcagggcccttaggcctgtttgccttttgaacttgacacgagcagtca tcaacagactttaatgaggccattgagtagcttgtgcacttttatatattctagcaacttctaggtttctatgagggtgacataatgtgcacatggtaaaaaaaaaaaaaacaaaaaccc agaaataattaaatagatgagggattatattaagcttgcttccatttctaaagaaataggttggggtgacttatttaaacattgacttttaaaaattacacagattatacagtcacaaaagta aatagcttcattgaacaaagaaaacagaaacaatgtgtgattttattgttcggagaaaactacttttaggttttggaatggggaggggtagtctctgtcaattgcttcttcctgttgaccaa gatcctctctgtcttgcaaagaatgggtatcccctgccggaccttcctcggtggctgtcaggctttgtgaaggaaggtctgaggatgtcaagaattttcagagcacagctattgctgac cctctgtttctattgatccgcctcctgaggttttgacctcaagtaaccttgagggagctgtctcctggctcggcatatttcttgtttagttatgagagacattcatctccccaacatttctgttt tgaatactttgaagatagcaatacaatttatggatgagactcaagcaggggttttgagtcagttaggaagtcacagttgattctcaggttgtgtttaagttatattcactgacatttctaac ctcttcaatctgatctcattatggttgtggttttttttaatttttattttattattattttttattaaatctctaatccttcaagtccagtccagcactgaactgttcccaaggtccctacatcaaaca ttccagagagtcctactattgctctattgaactatggaatttggtgatcagagcattccacaatagatccaagtttgtagatggaggatatctttcatgatagtaactctagcagaggtaaa agtcagcacagactgccaaaactggacatttgtttgcggtttactgtgtttcagaaatttagtacacagcatgctctggtggtggccaatgaattctaggacattccaaagagacatcag taatgaccaagcgtgctggcaagccctggagaagagggtagcctgggatgtagttgtctggtggttccagtaatcacaggcttttctttcttctggcagCCCCCAGTCCCC AGTCAGACCTCGTCATACTCGTGCATGCTGCCCGCCCGCCCGTCAGTGAATGGTCGGAGTTATGATACCTAC GCCCCTCCGCACATGCAAACACACATGAACAGTCAGCCCATGGGCACCTCGGGGACCACTTCAACAGgtgagct ctctgcagctgtgtagaggcatctactgggcctctttgaccagctgatctttcacactgtgtttcctattgtcttgaagagaaacttctgaccttgcattcaggactgtgttgaatattttact actcttgtcttgaaagaaaacagactgaatagggaaattcagttaagttagcgcgttgacagcatatagacaaatcatcgcttatggtggtaaatgtgatcacagagacagagtatgg agacaagaacccaaatcacgttttcagatgatatcttagtcagagctggacagtgagggtccactgaacttttgatgtgatgggtacttttagaaggcgttcacatcttctagcttcttga tgccagctgaggagtggagaagttaggtctggttttccacccagcccattttggcttctgaggatgtagcatgttagtcttccagagatggttgcactaaaaaacttccaaacattgg gtatcatgaggtacttgcaaacatagcctcgagtttcaaaaggtctgcttttcttttctaattgttgaaagttttcttttcttttcttttcttttcttttcttttcttttcttttcttttcttt cttttttataaagtaaaaaccatattatgaagtgttaggaattttagaaggtctgtgtgttcatgctgtgttctatcgtagaatctacctatgcggatggtgtttgaattttagaaagtctgtgtg ttcgcgccgtgttctattgtagaatgtacctatgcagctgttattgtattcatttatagGACTCATTGCACCTGGAGTGTCAGTTCCCGTGCAAGTTC CCGGGAGTGAACCTGACATGTCTCAGTACTGGCCTCGATTACAGTAAAGAGAGAAGGAGAGAGCATGTGAT CGAGAGAGGAAATTGTGTTCACTCTGCCAATGACTATGTGGACACAGCAGTTGGGTATTCAGGAAAGAAAG AGAAATGGCGGTTAGAAGCACTTCACTTTGTAACTGTCCTGAACTGGAGCCCGGGAATGGACTAGAACCAA GGACCTTTGCGTACAGAAGGCACGGTATCAGTTGGAACAAATCTTCATTTTGGTATCCAAACTTTTATTCATT TTGGTGTATTATTTGTAAATGGGCATTGGTATGTTATAATGAAGAAAAGAACAACACAGGCTGTTGGATCGC GGATCTGTGTTGCTCATGTGGTTGTTTAAAGGAAACCATGATCGACAAGATTTGCCATGGATTTAAGAGTTTT ATCAAGATATATCAAATACTTCTCCCCATCTGTTCATAGTTTATGGACTGATGTTCCAAGTTTGTATCATTCCT TTGCATATAATTGAACCTGGGACAACACACACTAGATATATGTAAAAACTATCTGTTGGTTTTCCAAAGGTT GTTAACAGATGAAGTTTATGTGCAAAAAAGGGTAAGATATGAATTCAAGGAGAAGTTGATAGCTAAAAGGT AGAGTGTGTCTTCGATATAATACAATTTGTTTTATGTCAAAATGTAAGTATTTGTCTTCCCTAGAAATCCTCA GAATGATTTCTATAATAAAGTTAATTTCATTTATATTTGACAAGAATACTC
Primer P1	tagtgaactctccgccgtct
Primer P2	GGTGGCAAAGCACTGTACG
Primer P3	ggtttgcaaagactcccttg
Primer P4	tcagcacagactgccaaaac

Primer P5	TGTGCTTCTTCGCAAATGAC
Primer P6	caaagaggcccagtagatgc
Primer P7	tggcttctgaggatgtagca
Primer P8	TACGCAAAGGTCCTTGGTTC

*, red and underlined nucleotides are the interesting nucleotides in seven phosphorylation-site substitution mutations; black and underlined nucleotides are the interesting nucleotides in PAM-site mutations.

Table 6. Sequence information of the material in generating *Pax6* all-site mutation transgenic mice via mouse stem cells

Name	Sequence
SgRNA-2	TACCAGGTGTGGTGGGCTGT
SgRNA-4	CCACCAGCCCGTCAGTGAAT
Repair template with Noemycin-resistant gene*	cagagaaaccttaaatcaaaggaaatgccacagcaaaagcacaaagggctaaatttagctagggctctttgcataaaggatgaaaagccccccccccccactttcagtgtgtgtgtttttttttttttgtgtgtgtgtgtgtgcgcgcatatgcattttctctctctttctcacacaccagcaaactgaaatattacaattctgacagacaaaggaaatgatgacctatctgactgtcttaggccacagataaggacaaacactaaatgtcattccaaagaaaacttgctcctggtgggaaagttcttgctagtacagtcagcacactgtcaagctgtctgattggctggatgagatgggagttgggtgttaaaagctaggttgatccagtgtctgaactatcttgtgttctggtataatatataaaatcaacttactctttcagAGTTTGAGAGGACCCATTATCCAGATGTGTTTGCCCGGGAAAGACTAGCAGCCAAAATAGATCTACCTGAAGCAAGAATACAGgtacctagggaccatgtggttttatgcactgggatgcttatattttgccttggctgtataccagtcactgatataatcatggtcaggtttgcaaagactcccttgttctagggtaagggtggggatggagggctttttgtttgtggccgagtggtagcaagcataggctaacctgttctgtgcatttccagGTATGGTTTTCTAATCGAAGGGCCAAATGGAGAAGAGAAGAGAAACTGAGGAACCAGAGAAGACAGGCCAGCAACGCTCCTAGTCACATTCCTATCAGCAGCAGCTTCAGTACCAGTGTCTACCAGCCAATTCCACAGCCCGCCGCACCTGgtaacttgaaatcccacctgccaagaaccgttcttaaccttgcctgcccttgacttttctcttgccttgtaatgaatgaccttgccctctctctgtctctttttctcttcctctgcagTCTCCTCCTTCACATCAGGTTCCATGTTGGGCCGAACAGACACCGCCCTCACCAACACGTACAGTGCTTTGCCACCCATGCCCAGCTTCACCATGGCAAACAACCTGCCTATGCAAgtaagagaggacggtcacctgctgcacagggcaagggatgggttcaggcttgcagaccccattcattgcatttactcccttgggagtccttcttgtgacagtgattagcttgaccagtcaactctgagacagtcaatccaacctcttttagctgattgattgactgattgattgattcatgcccttggaaaacaaacactctatctgttcagtcaagttaatgtgccttttcatcattatgttagctggagaaggccgggcgggcgggagtgaggtcgctttcggctaccagggatgtttgtatcaaagtagaaataattcgggcataatgaaaggtactaaagatgttggcatgtaaaaagtttaggtttacgttagtgggtttgtattaataaatgcagaagcagcacaaatattttggttccctctaagaagctagtgaggaagaggaaaaaggggaggggcagctgaaaagcaagattcctctttagagagtgaaatgcatttagtaaaataggaaactagctccttctacatttaaaagtaaaaatggagtagaaggtatttgctagaaatctaatgtgtgtcagctgtagccgatgtgacaggtcagtggtaaccccttgctgcctagggagctggagggcattcttcctataataccctggcccgtgttcttaggggttggttctggaccaagctggcatggcctagtgtaagttctgcatgactcctggtatgtgctagatcactgttgcttagaggattctgatgtcttaggaacatcagcaagtcctaaggctcctgctgtacgaccatcagatatgcctgctggtatacgactggaagcatgagccctgctggaagcagttcgggggaggggttctacagattactagcctgtactgaacatcttttgccaggcttggaattcaaataacagcaaaataaagtctctcagtcttcaggcctagaactggataagcggtgccggaggacatattccccctgcttctttctatggcatctgtctttttattggacatagtgcaactgatgtaaatgaaggggccagcagcccattaagtgggtatggctacaactattttggaatttcccagaagtcactttgcctagaggaagtgattgcaggaattagaagcaaatgcaagctgaagttctggcagggccctttaggcctgtttgccttttgaacttgacacgagcagtcatcaacagactttaatgaggccattgagtagcttgtgcactttttatatattctagcaacttctaggtttctatgagggtgacataatgtgcacatggtaaaaaaaaaaaaaaacaaaaacccagaaataattaaatagatgagggattatattaCTCGAGGTCGACGGTATCGATAAGCTTGATATCGAATTCCGAAGTTCCTATTCTCTAGAAAGTATAGGAACTTCAGGTCTGAAGAGGAGTTTACGTCCAGCCAAGCTAGCTTGGCTGCAGGTCGTCGAAATTCTACCGGGTAGGGGAGGCGCTTTTCCCAAGGCAGTCTGGAGCATGCGCTTTAGCAGCCCCGCTGGGCACTTGGCGCTACACAAGTGGCCTCTGGCCTCGCACACATTCCACATCCACCGGTAGGCGCCAACCGGCTCCGTTCTTTGGTGGCCCCTTCGCGCCACCTTCTACTCCTCCCCTAGTCAGGAAGTTCCCCCCCGCCCCGCAGCTCGCGTCGTGCAGGACGTGACAAATGGAAGTAGCACGTCTCACTAGTCTCGTGCAGATGGACAGCACCGCTGAGCAATGGAAGCGGGTAGGCCTTTGGGGCAGCGGCCAATAGCAGCTTTGCTCCTTCGCTTTCTGGGCTCAGAGGCTGGGAAGGGGTGGGTCCGGGGGCGGGCTCAGGGGCGGGCTCAGGGGCGGGGCGGGCGCCCGAAGGTCCTCCGGAGGCCCGGCATTCTGCACGCTTCAAAAGCGCACGTCTGCCGCGCTGTTCTCCTCTTCCTCATCTCCGGGCCTTTCGACCTGCAGCCTGTTGACAATTAATCATCGGCATAGTATATCGGCATAGTATAATACGACAAGGTGAGGAACTAAACCATGGGATCGGCCATTGAACAAGATGGATTGCACGCAGGTTCTCCGGCCGCTTGGGTGGAGAGGCTATTCGGCTATGACTGGGCACAACAGACAATCGGCTGCTCTGATGCCGCCGTGTTCCGGCTGTCAGCGCAGGGGCGCCCGGTTCTTTTTGTCAAGACCGACCTGTCCGGTGCCCTGAATGAACTGCAGGACGAGGCAGCGCGGCTATCGTGGCTGGCCACGACGGGCGTTCCTTGCGCAGCTGTGCTCGACGTTGTCACTGAAGCGGGAAGGGACTGGCTGCTATTGGGCGAAGTGCCGGGGCAGGATCTCCTGTCATCTCACCTTGCTCCTGCCGAGAAAGTATCCATCATGGCTGATGCAATGCGGCGGCTGCATACGCTTGATCCGGCTACCTGCCCATTCGACCACCAAGCGAAACATCGCATCGAGCGAGCACGTACTCGGATGGAAGCCGGTCTTGTCGATCAGGATGATCTGGACGAAGAGCATCAGGGGCTCGCGCCAGCCGAACTGTTCGCCAGGCTCAAGGCGCGCATGCCCGACGGCGATGATCTCGTCGTGACCCATGGCGATGCCTGCTTGCCGAATATCATGGTGGAAAATGGCCGCTTTTCTGGATTCATCGACTGTGGCCGGCTGGGTGTGGCGGACCGCTATCAGGACATAGCGTTGGCTACCCGTGATATTGCTGAAGAGCTTGGCGGCGAATGGGCTGACCGCTTCCTCGTGCTTTACGGTATCGCCGCTCCCGATTCGCAGCGCATCGCCTTCTATCGCCTTCTTGACGAGTTCTTCTGAGGGGATCAATTCTCTAGAGCTCGCTGATCAGCCTCGACTGTGCCTTCTAGTTGCCAGCCATCTGTTGTTTGCCCCTCCCCCGTGCCTTCCTTGACCCTGGAAGGTGCCACTCCCACTGTCCTTTCCTAATAAAATGAGGAAATTGCATCGCATTGTCTGAGTAGGTGTCATTCTATTCTGGGGGGTGGGGTGGGGCAGGACAGCAAGGGGGAGGATTGGGAAGACAATAGCAGGCATGCTGGGGATGCGGTGGGCTCTATGGCTTCTGAGGCGGAAAGAACCAGCTGGGGCTCGACTAGAGCTTGCGGAACCCTTCGAAGTTCCTATTCTCTAGAAAGTATAGGAACTTCATCAGTCAGGTACATAATATAACTTCGTATAATGTATGCTagcttgcttccatttctaaagaaataggttggggtgacttatttaaacattgacttttaaaaattacacagattatacagtcacaaaagtaaatagcttcattgaacaaagaaaacagaaacaatgtgtgattttattgttcggagaaaactacttttttaggttttggaatggggaggggtagtctctgtcaattgcttcttcctgttgaccaagatcctctctgtcttgcaaagaatgggtatcccctgccggacctttcctcggtggctgtcaggctttgtgaaggaaggtctgaggatgtcaagaattttcagagcacagctattgctgaccctctgtttctattgatccgcctcctgaggtttttgacctcaagtaaccttgagggagctgtctcctggctcggcatatttcttgtttagttatgagagacattcatctcccccaacatttctgttttgaaatactttgaagatagcaatacaatttttatggatgagactcaagcagggggtttttgagtcagttagagaagtcacagttgattctcaggttgtgtttaagttatattcactgacatttctaacctcttcaatctgatctcattatggttgtggttttttttaatttttattttatttattttttattaaatctctaatccttcaagtccagtccagcactgaactgttcccaaggtccctacatcaaacattccagagagtcctactattgctctattgaactatggaatttggtgatcagagcattccacaatagatccaagtttgtagatggaggatatctttcatgatagtaactctagcagaggtaaaagtcagcacagactgccaaaactggacatttgtttgcggtttactgtgtttcagaaatttagtacacagcatgctctggtggtggccaatgaattctaggacattccaaagagacatcagtaatgaccaagcgtgctggcaagccctggagaagagggtagcctgggatgtagttgtctggtggttccagtaatcacaggcttttctttcttctggcagCCCCCAGTCCCCAGTCAGACCTCGTCATACTCGTGCATGCTGCCCGCCGCCCCGTCAGTGAATGGTCGGAGTTATGATACCTACGCCCCTCCGCACATGCAAACACACATGAACAGTCAGCCCATGGGCACCTCGGGGACCACTTCAACAGgtgagctctctgcagctgtgtagaggcatctactgggcctctttgaccagctgatctttcacactgtgtttcctattgtcttgaagagaaacttctgaccttgcattcaggactgtgttgaatatttttactactcttgtcttgaaagaaaacagactgaatagggaaattcagttaagttagcgcgttgacagcatatagacaaatcatcgcttatggtggtaaatgtgatcacagagacagagtatggagacaagaacccaaatcacgttttcagatgatatctttagtcagagctggacagtgagggtccactgaacttttgatgtgatgggtacttttttagaaggcgttcacatcttctagcttcttgatgccagctgaggagtggagaagttaggtctggtttttccaccc agccccattttggcttctgaggatgtagcatgttagtcttccagagatggttgcactaaaaaacttccaaacattgggtatcatgaggtacttgcaaacatagcctcgagtttcaaaaggtctgctttttctttctaattgttgaaagttttcttttcttttcttttcttttcttttcttttcttttcttttcttttcttttcttttttttataaagtaaaaaccatattatgaagtgttaggaatttagaaggtctgtgtgttcatgctgtgttctatcgtagaatctacctatgcggatggtgtttgaattttagaaagtctgtgttgcgcgccgttgtttcattgtagaatgtacctatgcagctgttattgtattcatttatagGACTCATTGCACCTGGAGTGTCAGTTCCCGTGCAAGTTCCCGGGAGTGAACCTGACATGTCTCAGTACTGGCCTCGATTACAGTAAAGAGAGAAGGAGAGAGCATGTGATCGAGAGAGGAAATTGTGTTCACTCTGCCAATGACTATGTGGACACAGCAGTTGGGTATTCAGGAAAGAAAGAGAAATGGCGGTTAGAAGCACTTCACTTTGTAACTGTCCTGAACTGGAGCCCGGGAATGGACT

	AGAACCAAGGACCTTTGCGTACAGAAGGCACGGTATCAGTTGGAACAAATCTTCATTTTGGTATCCAAACTTTTATTCAT TTTGGTGTATTATTTGTAAATGGGCATTGGTATGTTATAATGAAGAAAAGAACAACACAGGCTGTTGGATCGCGGATCTG TGTTGCTCATGTGGTTGTTTAAAGGAAACCATGATCGACAAGATTTGCCATGGATTTAAGAGTTTTATCAAGATATATCA AATACTTCTCCCCATCTGTTCATAGTTTATGGACTGATGTTCCAAGTTTGTATCATTCCTTTGCATATAATTGAACCTGGG ACAACACACACTAGATATATGTAAAAACTATCTGTTGGTTTTCCAAAGGTTGTTAACAGATGAAGTTTATGTGCAAAAAA GGGTAAGATATGAATTCAAGGAGAAGTTGATAGCTAAAAGGTAGAGTGTGTCTTCGATATAATACAATTTGTTTTATGTC AAAATGTAAGTATTTGTCTTCCCTAGAAATCCTCAGAATGATTTCTATAATAAAGTTAATTTCATTTATATTTGACAAGAA TACTC

*, red and underlined nucleotides are the interesting nucleotides in seven phosphorylation-site substitution mutations; black and underlined nucleotides are the interesting nucleotides in PAM-site mutations.

Table 7. Sequence information of the material in generating *Pax6*-null and *Pax6*-phosphorylation-site mutation 21EM15 cell Lines

Name	Sequence
Sg-RNA8	TCGTAGAGCTAGCTCACAGC
Primer P1	TCAGCTTGGTGGTGTCTTTG
Primer P2	GGGGAAAGCTGGAAGGTAAG
Primer P3	GAAGGAGGGGGAGAGAACAC
Primer P4	ACTTGGACGGGAACTGACAC

Table 8. *Pax6*-null 21EM15 cell lines

Clone#	mutation
D8	36bp-deletion, in-frame mutation on both alleles
F9	44bp-deletion, causing pre-mature mutation on both alleles
B7	about 61bp deleted on both alleles